Journal of Fluid Mechanics and Engineering

Volume No. 8

Issue No. 1

January - April 2024

ENRICHED PUBLICATIONS PVT. LTD

S-9, IInd FLOOR, MLU POCKET,
MANISH ABHINAV PLAZA-II, ABOVE FEDERAL BANK,
PLOT NO-5, SECTOR-5, DWARKA, NEW DELHI, INDIA-110075,
PHONE: - + (91)-(11)-47026006

Journal of Fluid Mechanics and Engineering

Aims and Scope

Journal of Fluid Mechanics is a peer reviewed journal published by Enriched Publication and papers describing significant developments in computational methods that are applicable to scientific and engineering problems in fluid mechanics, fluid dynamics, micro and bio fluids, and fluid structure interaction. Numerical methods for solving ancillary equations, such as transport and advection and diffusion, are also relevant. This journal consist of research articles and theoretical articles are also accepted of this subject

Journal of Fluid Mechanics and Engineering

Journal of Fluid Mechanics and Engineering

(Volume No. 8, Issue No. 1, January - April 2024)

Contents

Fabrication of Al6082/ZrO_2 Surface Composite by Friction Stir Processing

N. Yuvaraj* and Vipin
Department of Mechanical Engineering, Delhi Technological University, Delhi 110 042, India
* e-mail: yuvraj@dce.ac.in
Tel:+91987153668

A B S T R A C T

Nowadays surface composites are given more attention in fabrication of service life of the components. In this present work, Friction stir processing (FSP) was used to fabricate the surface composite on Al6082 alloy with ZrO_2 particles. Aluminum with four different volume % fractions of ZrO_2 reinforcement particles were used to synthesize the composite. The microhardness and tensile properties of the surface composites and base alloy were investigated. Microstructural observations and fractured tensile surface of the composite layer were studied using Scanning Electron Microscope. The results show that the hardness and tensile strength of the composite produced by 15 % ZrO_2 composite was higher than other volume percentage of ceramic surface composites.

Keywords- Friction stir processing (FSP); ZrO_2: Tensile; Hardness

1. INTRODUCTION

The conventional aluminum alloys does not provide the sufficient properties under all service conditions, which are overcome by reinforcing those alloys with ceramic particles. Aluminum based Metal Matrix Composites are used in automotive, aircraft and structural applications. Various methods are used for fabricating the Aluminum matrix composites such as Thermal Spraying, Laser Beam Techniques, Powder metallurgy, stir casting, pressure less infiltration, squeeze casting, and compo casting [1-2]. All these methods are difficult to reinforcing the ceramic particles in the matrix due to poor bonding between reinforcement and matrix. Recently great attention has been paid for the new composite fabricating technique named friction stir processing based on the Friction stir welding (FSW) [3]. In the FSP process, the rotating tool non consumable tool with shoulder and specially designed tool pin is inserted in a work piece. The heating is accomplished by friction between the tool shoulder and the work and pin causes intense stirring of the material. The localized heating softens the material around the pin and translation leads to movement of material from the front of the pin to the back of the pin causes intense stirring of the matrix and reinforcement material. M. Salehi et al. [4] studied the process parameters for producing Al6061/SiC composites by FSP method and found that

rotational speed is most influential parameter. A. Devaraju et al. [5] found that the SiC and Graphite particles are greatly influenced on wear & mechanical properties of aluminum hybrid composites via FSP. S. Shahraki et al. [6] reported that rotational speed and traverse speed of the FSP are greatly influenced for fabrication of Al5083/ZrO2 surface composites. F. Khodabakhshi et al. [7] reported that the hardness and yield strength of FSPed Al-Mg/TiO_2 surface composites was increased with increasing the volume fraction of TiO_2 particles in the composites. C. Maxwell Rejil et al. [8] reported that FSP of Al6360/TiC/B_4C composite surface layer has lower wear rate than base material. Both the TiC and B_4C particles behaved as one type of reinforcement particles which is difficult to be achieved by conventional liquid processing route due to segregation. N. Yuvaraj et al. [9] studied the effect of number of passes on the surface nano composite fabricated through FSP technique. A. Thangarasu et al. [10] studied the effect of different volume content of TiC particles in the Al6082/TiC composite and found that with increase in TiC particles the hardness of the composite was increased. Zirconium di boride (ZrO_2) ceramics have a high melting point, high hardness, high electrical conductivity, excellent corrosion resistance and excellent thermal shock resistance [11]. In the present study, FSP technique is used to fabricate the Al6082/ZrO_2 surface composite. The effects of hardness and tensile properties of the surface composite were investigated.

2. MATERIALS AND METHODS

Al6082-T6 alloy of 6 mm thickness and commercially available ZrO_2 powder size of 10μm were used as substrate and particulates. The chemical composition (%) of the base metal is 1.2Si, 0.78Mn, 0.75Mn, 0.4Fe, 0.15Cr and rest Al. The plates were cut into rectangular pieces of 180 mm×80 mm×6 mm. Four different groove width sizes of 0mm, 0.5mm, 1.0mm and 1.5mm & constant 3mm depth of four such plates were prepared, in order to get the different volume fraction (0, 5, 10% and 15%) of the particles in the composite. The volume fractions of the particles are calculated based on the formula mentioned below [12].

$$Theoretical\ Volume\ fraction\ (Vt) = \frac{Area\ of\ groove}{Projected\ area\ of\ the\ tool\ pin}\ x\ 100 \ldots (1)$$

$$Area\ of\ groove = Groove\ width\ x\ depth \ldots\ldots\ldots\ldots\ldots\ldots\ldots\ldots (2)$$

$$Projected\ area\ of\ tool\ pin = pin\ diameter\ x\ pin\ length \ldots\ldots\ldots\ldots\ldots (3)$$

The particles were mixed with acetone and packed on the groove tightly. Then the substrates were fixed in the hydraulic fixture of the FSW machine (11 kW& 40KN). Fig. 1 shows the typical FSP experimental setup.

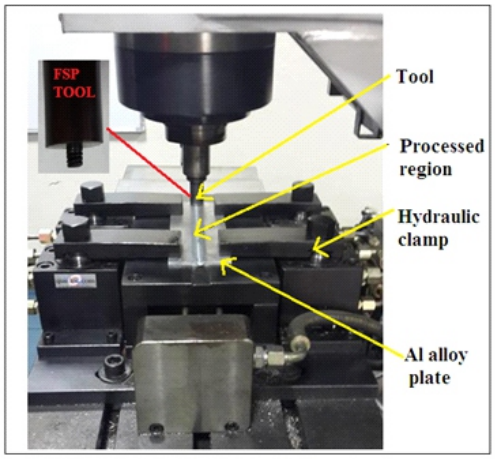

Figure 1. FSP Experimental setup

Non-consumable cylindrical threaded tool made of H-13 steel were used to perform the FSP. The shoulder diameter, pin diameter and pin length were 18 mm, 6 mm and 5mm respectively. The shoulder tilt angle was fixed at 1°. In order to prevent scattering of ZrO_2 powder and its ejection from groove during the process, groove's gap initially was closed with pinless tool. Three FSP passes were carried out for uniform mixing of the reinforcement particles in the matrix.

The tensile specimens were extracted from the surface composites along the FSP direction as per ASTM: E8/E8 M-011 standard by wire cut electrical discharge machining. Figure 2 (a) shows the tensile specimen extracted from the FSP region and (b) shows the schematic sketch of tensile specimen. The tensile test was conducted with universal testing machine (Tinius Olsen H50KS) at strain rate 1mm/min. Hardness testing was carried out on Microhardness tester with test load of 100 gm and dwell time of 10 sec. Micro structural characterization was observed on Scanning Electron Microscope (SEM) (Hitachi S3700).

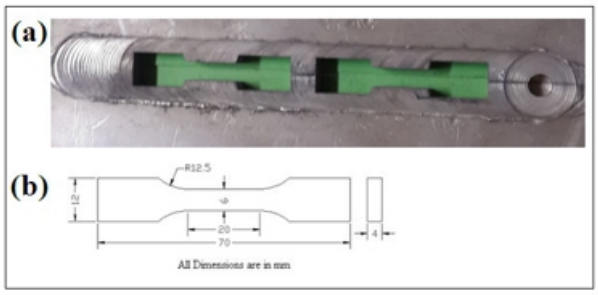

Figure 2. (a) Tensile specimen extracted from the FSP region and (b) Schematic sketch of tensile specimen.

3. RESULTS AND DISCUSSIONS

Hardness

Figure 3 shows the SEM images of the different percentage of volume content of reinforcement composite samples. It clearly indicates that the ceramic particles are distributed in uniform and homogeneous manner in the matrix due to increase in FSP passes. Figure 4 shows the hardness values of the cross section of the composite surface and base material. For experimental purpose, the average of three hardness value was taken for all the samples. The hardness of the 15% ZrO_2 specimen is higher than other Vol % of ZrO_2 composite samples. Composite sample exhibited increase in hardness by 37%, and the base material hardness was 80±2 Hv.

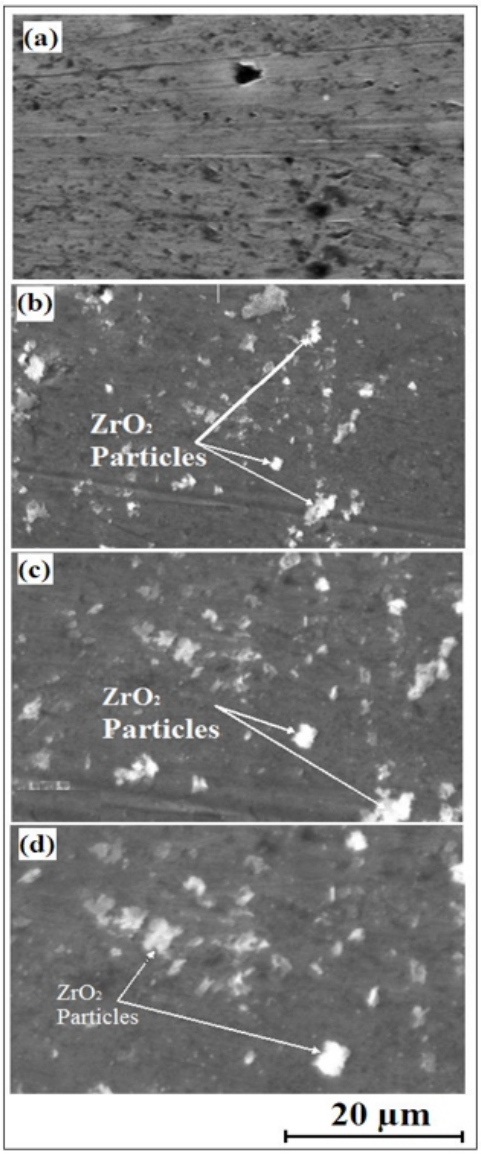

Figure 3 SEM micrograph of Al6082/ZrO_2 surface composite

There was an increase in microhardness of the friction stir processed composite as compared base alloy. This might be attributed to effective formation of refined grain structure due to the restrain of grain boundary and the enhancement of the induced strain. Similar types of results are reported by various researchers [13-14]. As per Hall petch relationship smaller grain size of the matrix has higher the hardness [15]. In addition uniform dispersion of reinforcement particles in the matrix and good bonding between the matrix and reinforcement enhances the hardness. With increase in number of passes and changing of tool direction between passes increases the good bonding of ceramic particles with matrix also responsible for enhancement of hardness.

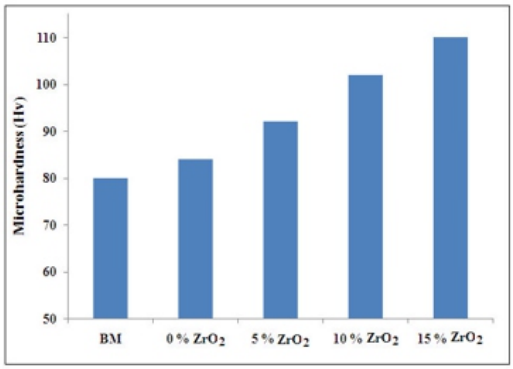

Figure 4. Effect of ZrO_2 (vol%) content on microhardness of Al6082/ZrO_2 surface composite

Tensile strength

Figure 5 shows the tensile results of the base alloy and composite samples. The 15% ZrO2 particles consists composite sample has the maximum tensile strength value of 340Mpa. Similar type of results reported for FSPed Al/6082/TiC composite samples [10]. The tensile strength is increasing with increase in % of ceramic particles. The major contributions for enhancement of the mechanical properties of the surface composite is due to fine grain size of matrix and load transfer from matrix to hard reinforcements. Figure 6 shows tensile tested sample factography of the base alloy and composite sample. In base material larger size of dimples observed, in the composite sample finer size of the dimples with some ceramic particles observed. It shows the composite sample having good tensile properties with finer refinement of grain size and dispersion of the reinforcements.

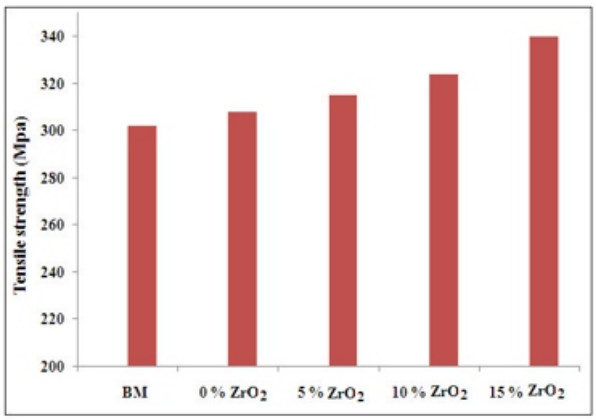

Figure 5. Effect of ZrO_2 (vol%) content on Tensile strength of Al6082/ZrO_2 surface composite

4. CONCLUSION

In this study the effects of reinforcement particles on hardness and tensile strength of Al/ZrO_2 surface composite were fabricated through FSP and the following conclusions can be drawn.

1. Al-ZrO_2 composite specimen exhibits with higher hardness and better tensile properties when compare to base material.
2. ZrO_2 particles are strengthened the Aluminum matrix composite. With increase in volume fraction of the reinforcement particles in the matrix the mechanical properties of the composite was increased.
3. The composite specimens contains 15% ZrO_2 has higher hardness of 110Hv and tensile strength of 340Mpa. Base material hardness and tensile strength were 80Hv and 302Mpa respectively.
4. Finer refinement of the grain size and uniform dispersion of reinforcement particles in the matrix are responsible for enhancement of mechanical properties of the composite.

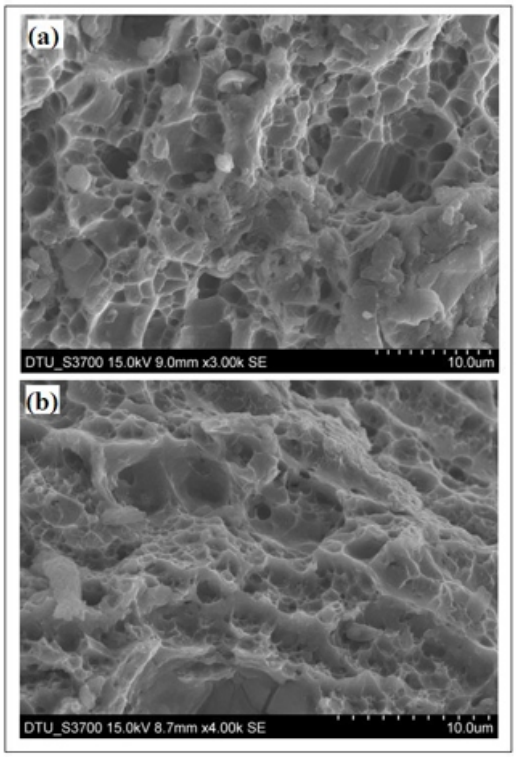

Figure 6. Tensile fractured surface of (a) Base Material (b) Al/15% ZrO2 surface composite

5. REFERENCES

[1] D.B. Miracle, (2005) "Metal matrix composites–From science to technological significance", Composites Science and Technology Vol. 65, pp. 2526–2540, 2005.
[2] A.V. Muley, S. Aravindan, and I.P. Singh, "Nano and hybrid aluminum based metal matrix composites: an overview", Manufacturing Review. Vol. 2, pp. 1-13, 2015.
[3] V. Sharma, U. Prakash, and B.V.M. Kumar, "Surface composites by friction stir processing: A review", Journal of Materials Processing Technology Vol. 224, pp. 117-134, 2015.

[4] M. Salehi, M. Saadatmand, and J. A. Mohandesi, "Optimization of process parameters for producing AA6061/SiC Nano composites by friction stir processing", Trans. Nonferrous Met. Soc. China, Vol. 22, pp 1055-1063, 2012.

[5] A. Devaraju, A.Kumar, and B. Kotiveerachari, "Influence of rotational speed and reinforcement on wear & mechanical Properties of aluminium hybrid composites via FSP", Materials and Design, Vol. 45, pp. 576–585, 2013.

[6] S. Shahraki, S. Khorasani, R.A. Behnagh, Y. Fotouhi, and H. Bisadi, "Producing of AA5083/ZrO_2 Nanocomposite by Friction Stir Processing (FSP)", Metallurgical and Materials Transactions B, Vol. 44, pp. 1546-1553, 2013.

[7] F. Khodabakhshi, A. Simchi, A.H. Kokabi, M. Nosko, F. Simancik, and P. Svec, "Microstructure and texture development during friction stir processing of Al-Mg alloy sheets with TiO_2nano particles", Materials Science and Engineering A, Vol. 605, pp. 108-118, 2014.

[8] C. M. Rejil, I. Dinaharan, S.J. Vijay, and N. Murugan, "Microstructure and sliding wear behavior of AA6360/(TiC + B_4C) hybrid surface composite layer synthesized by friction stir processing on aluminum substrate", Materials Science and Engineering A Vol. 552, pp. 336-344, 2012.

[9] N. Yuvaraj, S. Aravindan, and Vipin, "Fabrication of Al5083/B_4C surface composite by friction stir processing and its tribological characterization", Journal of Materials Research Technology, Vol. 4, pp. 398-410, 2015.

[10] A. Thangarasu, N. Murugan, I. Dinaharan, and S.J. Vijay, "Synthesis and characterization of titanium carbide particulate reinforced AA6082 aluminium alloy composites via friction stir processing", Archives of Civil and Mechanical Engineering, Vol. 15, pp. 324-334, 2015.

[11] H. Zhu, J. Min, Y.L. Ai, D.C.H. Wang, and H. Wang, "The reaction mechanism and mechanical properties of the composites fabricated in an Al–ZrO_2–C system". Materials Science and Engineering A, Vol. 527, pp 6178–6183, 2010.

[12] R. Sathiskumar, N. Murugan, I. Dinaharan, and S.J. Vijay, "Characterization of boron carbide particulate reinforced in situ copper surface composites synthesized using friction stir processing", Materials Characterization, Vol. 84, pp. 16 – 27, 2013.

[13] M. Amra, K. Ranjbar, and R. Dehmolaei, "Mechanical Properties and Corrosion Behavior of CeO_2 and SiC incorporated Al5083 Alloy Surface Composites", Journal of Materials and Engineering and Performance, Vol. 24, pp. 3169-3179, 2015.

[14] N. Yuvaraj, S. Aravindan, and Vipin, "Wear Characteristics of Al5083 Surface Hybrid Nano-composites by Friction Stir Processing", Trans. Ind. Inst. Met., DOI10.1007/s12666-016-0905-9, 2016.

[15] H. Izadi, R. Sandstrom, and A.P. Gerlich, Grain Growth Behavior and Hall–Petch Strengthening in Friction Stir Processed Al 5059, Metallurgical and Materials Transactions A, Vol. 45A, pp. 5635-5644, 2014.

Thermal Performance and Emission Test of CI Engine Using Biodiesel Produced from Waste Cooking Oil Blend With Diesel

Jatinder Kataria[1], S. K. Mohapatra[2], K. Kundu[3]

[1] Department of Mechanical Engineering, Thapar University, Patiala-147004, Punjab, India, Jatinder80@gmail.com,

[2] Department of Mechanical Engineering, Thapar University, Patiala-147004, Punjab, India Second skmohapatra@thapar.edu

[3] Department of Bio fuel, Centre of Excellence for Farm Machinery, Ludhiana -141006, Punjab, India K_kundu@cmeri.res.in

[‡] Corresponding Author; Tel: +9996919882

ABSTRACT

Compression ignition (C.I.) engine is the undebated choice for power applications, stationary or mobile. There is an urgent need of alternative high potential fuel for C.I. engines in order to fulfil energy needs without hampering the thermal performance and stringent emission standards. In the present work, a four stroke variable compression ratio engine was tested. Waste cooking oil was chosen as an alternative fuel, which was upgraded into biodiesel in the laboratory using mechanical stirring and ultrasonic cavitation technique of biodiesel production. The various biodiesel blends were prepared (i.e. B20, B40, B60, B80 and B100) with conventional diesel fuel and two compression ratios (i.e. 15, 17.5) were chosen for present work. The experimental test rig including hardware interfaced with engine soft software was used for online data logging for thermal performance of engine in tabulated and graphical form. The emission of CO, HC, and NOx were measured using AVL gas analyser (AVL Di gas 444), while smoke opacity was recorded using AVL 437. The thermal and engine emissions were obtained in the laboratory for different concentration of biodiesel blends at two compression ratios (i.e. 15, 17.5) for comparative analysis. The results showed that as the biodiesel concentration in a blend was increased, the thermal performance and emission were observed to be marginally higher; on the other hand as compression ratio was increased, the thermal performance improved, CO and smoke opacity decreased, while HC and NOx level increased.

Keywords- Compression ignition engine; waste cooking oil; mechanical stirring; ultrasonic cavitation,; smoke opacity; thermal performance

1. INTRODUCTION

In the present context, compression ignition engines are the undebated choice for almost all shaft power (stationary or mobile) applications. The massive utilization of diesel fuel due to their superior fuel economy and robustness has resulted in diesel crisis, in addition to environment threat leading to climate change. From a survey, the world consumption for petroleum and other liquid fuels is expected to reach at 107 million barrel per day by 2030 [1]. The globe today uses about 147 trillion kWh of energy which is expected to rise in the coming future [2]. Under such exponentially increasing trend, it can be realized that the petroleum resources might be depleting fast. A major chunk of this exponential rise in energy demand will be due to the developing countries, which is bound to grow leaps and bounds.

Another major global concern is environmental degradation. The intergovernmental panel on climate change (IPCC) concluded in "climate change- 2007" that because of global warming effect the global surface temperatures are likely to increase by 1.1^0C to 6.4^0C between 1990 and 2100. Due to these two reasons the whole world is in the search of an alternative fuel which is similar to the conventional diesel in terms of physical and chemical properties and can be used in the existing diesel engine without any engine modifications. Biodiesel is biodegradable, renewable and environment- friendly [3].

1.1 Biodiesel fuel

The idea of utilization of vegetable oil as substitute for diesel was demonstrated by Rudolph Diesel around the year 1900, when vegetable oil was proposed as fuel for engines. Various products derived from vegetable oils have been proposed as an alternative fuel for diesel engines [4]. Biodiesel can be produced from an enormous feedstock such as vegetable oils or animal fats [5].Vegetable oils may be edible or non-edible. Previously, the use of vegetable oil as diesel fuel was limited due to its high viscosity (near 10 times of the gas oil) [6]. In order to adapt the fuel to the existing engine the properties of vegetable oil had to be modified. The increased viscosity and low volatility of vegetable oils for diesel engine lead to severe engine deposits, injector choking and piston ring sticking [7]. However, these effects can be minimised or eliminated through transesterification process of vegetable oil to form methyl ester [8]. Transesterification will reduce the viscosity up to the level of conventional diesel and will make the fuel suitable for engine operations. Transesterification is the process of reacting a triglyceride with an alcohol in the presence of a catalyst to produce glycerol and fatty acid esters. The whole process is shown in fig1.

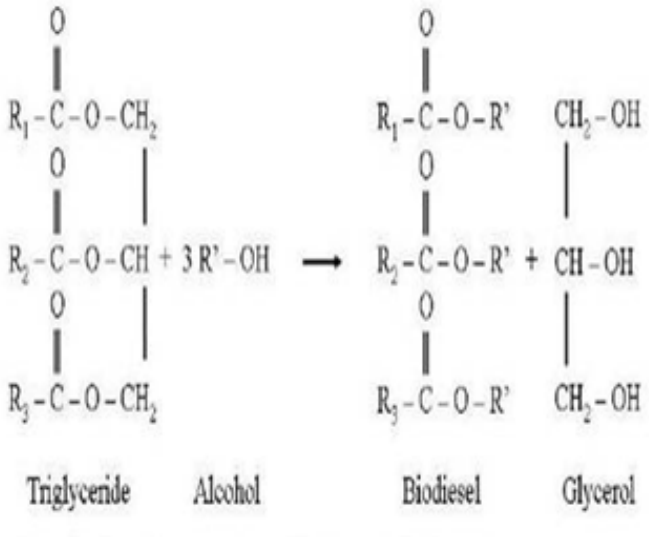

Fig-1. Transesterification Process

ASTM international defines “Biodiesel as the mono alkyl esters of long chain fatty acids derived from renewable liquid feedstock such as vegetable oils and animal fats for use in CI engines”. Biodiesel can be blended in any proportions with petroleum diesel or can be used neatly. The use of biodiesel in conventional diesel engines results in substantial reduction in all emissions except NOx which can be controlled by EGR [9]. Biodiesel differs from conventional diesel fuel in its chemical and thermophysical properties which results in the difference in its combustion characteristics. For instance, the cetane number of biodiesel is higher than conventional diesel which leads to the shorter ignition delay time. The viscosity of biodiesel is higher approximately 1.5 times than conventional diesel [10] and due to larger viscosity the combustion duration of biodiesel is higher. On account of high kinematic viscosity; nozzle fuel spray, evaporation and atomization process of biodiesel results in slower burning and longer combustion duration [11], despite the duration is shorter than conventional diesel under low, medium and high load [12]. The cold flow properties such as cloud point and the pour point are also greater than conventional diesel. Due to this, it is less responsive in cold weather which results in difficult starting in cold weather. The heat release rate of biodiesel is lower than conventional diesel, lessening the peak pressure rise rate, peak cylinder pressure and power. It is estimated that in current scenario, as compared to conventional diesel the cost of biodiesel is higher, which is the main hindrance to its commercialization. 70%-85% of the total biodiesel production cost arises from the cost of raw material [13]. Using waste cooking oil as raw material should reduce the raw material cost and make it competitive in price with conventional diesel. Waste cooking oil thus opened a good opportunity to study its suitability to produce biodiesel. Thus the main aim of this work was to investigate the physical and chemical characteristics of waste cooking oil and compare these properties with base line diesel for thermal and emission performance. The properties of the base line diesel and waste cooking methyl ester are given in table 1.

Item	Units	ASTM STANDARDS	DIESEL	Biodiesel	ASTM Methods
Cetane Number	--	--	50.88	51.34	ASTM D 4737
Lower Heating value	MJ/Kg	--	42.98	38.85	ASTM D3338
Density	kg/m^3		820	878	ASTM D 1298
Kinematic Viscosity	cst	<5	2.049	3.57	ASTM D445
Flash Point	C	>130	60	90	ASTM D93
Fire Point	C	>53	67	150	---------
Calorific value	kJ/kg	>33000	42000	39543	----------

Table-1. Properties of diesel and waste cooking oil methyl ester

2. EXPERIMENTAL SETUP

Experimental setup consisted of variable compression ratio compression ignition engine of 3.5 kW rated power single cylinder vertical water cooled engine connected to eddy current dynamometer for loading. This setup enabled varying the compression ratio for measurement of engine's thermal performance parameters (i.e., brake power, indicated power, frictional power, BMEP, IMEP, brake thermal efficiency, indicated thermal efficiency, mechanical efficiency, volumetric efficiency, specific fuel consumption, A/F ratio) using engine performance analysis software package "Engine Soft LV". A set of piezoelectric sensors were mounted on the engine for pressure measurements. One mounted on cylinder head, was for measuring cylinder pressure and the other was mounted on the fuel line near the injector for measuring injection pressure. The piezo sensors have an advantage of good frequency response and linear operating range. Specially designed tilting cylinder block arrangement mechanism was used for varying the compression ratio without stopping the engine and without altering the combustion chamber geometry. The compression ratio could not be brought below 13 because of knocking and greater vibration. A small water pump was used for continuous flow of water for cooling the engine and its associated parts. An eddy current dynamometer was used for loading the engine. The dynamometer consisted of a rotor mounted on a shaft running in bearings, which rotates within a casing. Inside the casing, there were two field coils connected in series. When these coils were supplied with a direct current, a magnetic field was created in the casing on either side of the rotor. When the rotor was turned in this magnetic field, eddy currents were induced creating a braking effect between the rotor and casing. The rotational torque exerted on the casing was measured by a strain gauge load cell incorporated in the restraining linkage between the casing and dynamometer bedplate. To prevent overheating of the dynamometer, water was circulated through the casing using a pump. The setup consisted of transmitters for air and fuel flow measurements. Rota meters were provided for cooling water and calorimeter water flow measurement. Provision was also made for online measurement of temperature of exhaust, inlet, and outlet cooling water and calorimeter water flow rate and load on the engine. These signals were interfaced to a computer through a data acquisition system. Windows based engine performance analysis software package "Engine soft LV" was used for online performance evaluation. The software displays P- φ and P-V diagrams, power, mean effective pressure, thermal efficiency, specific fuel consumption, air-fuel ratio, and heat utilized. The exhaust gases from the engine were sampled from exhaust line through a specially designed arrangement for diverting the exhaust gas through sample line without increasing the back pressure and was then analysed using exhaust gas analyser. The gases measured were CO (% and ppm), CO_2 (%), HC (ppm), O_2 (%), NOx (ppm), and SOx (ppm). For measurement of smoke intensity of the exhaust gas, a smoke meter was used. The smoke intensity was measured in terms of Hartridge Smoke Unit (%). The instrument also measured the absorption coefficient K of the exhaust gas in m^{-1}.The specifications of the engine used for conducting the experiments are as given in Table 2.

Table-2. Test Engine Specification

Engine Type	Variable compression ratio 4 stroke Compression ignition engine
Number of cylinders	One
Bore and stroke	87.5 X 110 mm
Compression ratio	12 to 18
Swept volume	661cc
Rated power	3.5 kW @ 1500 rpm
Fuel injection timing	24^0 BTDC
Type of injection nozzle	Pintle
Number of nozzle	1
Nozzle hole diameter	0.25 mm

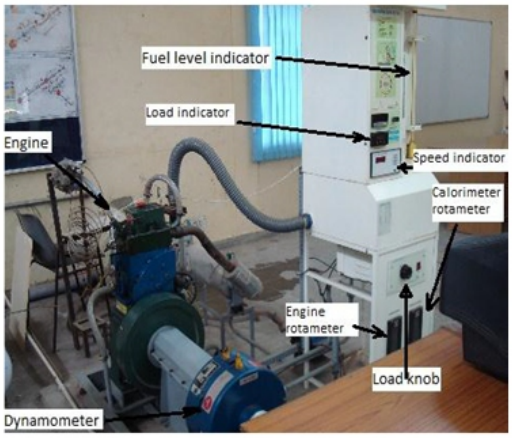

Fig-2. Photographic view of VCR CI Engine

3. EXPERIMENTAL PROCEDURE

The experiment was conducted for pure diesel, blends of biodiesel from waste cooking oil with diesel and, pure biodiesel from waste cooking oil which is termed as B100. BXX is the general term used for blend where XX signifies the percentage of biodiesel in the blend. For example a blend of 20% biodiesel and 80% diesel the designation is B20. The experiments were performed for diesel, B20, B40, B60, B80, and B100. Before cranking the engine, a sufficient amount of lubricating oil and fuel was ensured. The water flow was set at 250 LPH and calorimeter to 60 LPH. The computer was powered ON and ENGINESOFT LV was started and the calorific value, density of fuel and compression ratio were entered. Now the engine was cranked manually and made to run ideally for 5 min. When the engine reached its stabilized conditions, the readings were recorded at different loading conditions such as no load, part load and full load. For changing the compression ratio, tilting cylinder head mechanism was used which is user- friendly. By loosening the Allen bolts, the block was tilted by using the adjuster screw to a particular compression ratio. After attaining the desired compression ratio, the Allen bolt was tightened. The range of compression ratio was varied from 14 to 18 and injection pressure 150 bar to 250 bar.

The thermal performance of the engine was evaluated in terms of brake-specific fuel consumption (BSFC) and brake thermal efficiency (BTHE), and the emissions measured were carbon monoxide,

carbon dioxide, unburnt hydrocarbon, oxides of nitrogen, oxides of sulfur, and oxygen. The smoke intensity and absorption coefficient of exhaust gas were also measured.

4. RESULTS AND DISCUSSIONS

Various engine performance parameters such as brake thermal efficiency, specific fuel consumption, mechanical efficiency and engine emission parameters such as carbon monoxide, unburnt hydrocarbon, nitric oxide and smoke opacity were measured at two compression ratios (i.e. 15:1 and 17.5:1) for all blends of biodiesel along with diesel at different engine loads.

4.1 BRAKE SPECIFIC FUEL CONSUMPTION (BSFC)

The effect of variation of brake power output on specific fuel consumption at typical compression ratios of 17.5 and 15 for different biodiesel blends are shown in figure 4.1-4.3. The specific fuel consumption decreases with brake power output. It can be observed that specific fuel consumption does not show any significant deviation with different blends of biodiesel fuel. The effect of compression ratio has been highlighted in fig 3. It shows marginally lower specific fuel consumption at higher compression ratio. It can be observed that for all blends of biodiesel, the brake specific fuel consumption was higher than conventional diesel. This pattern was due to the fact that biodiesel blends have a lower heating value than does conventional diesel. We can also see that the BSFC of B20 is almost the same as that of base line diesel at both compression ratios (17.5 and 15 respectively).

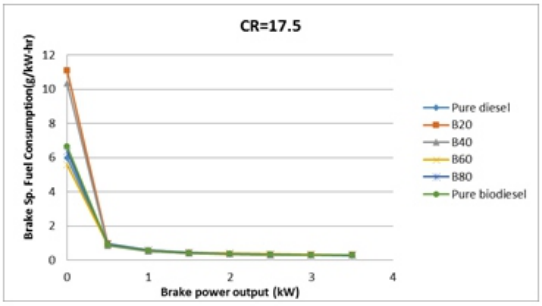

Fig-4.1. Brake specific fuel consumptions v/s Brake power (CR 17.5)

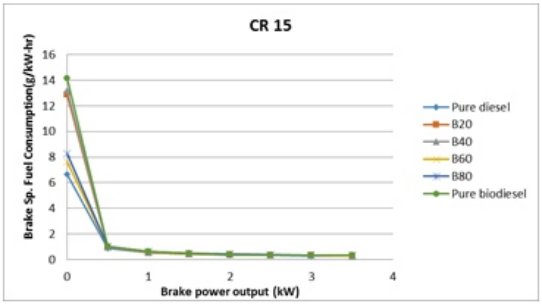

Fig-4.2. Brake specific fuel consumptions v/s Brake power (CR 15)

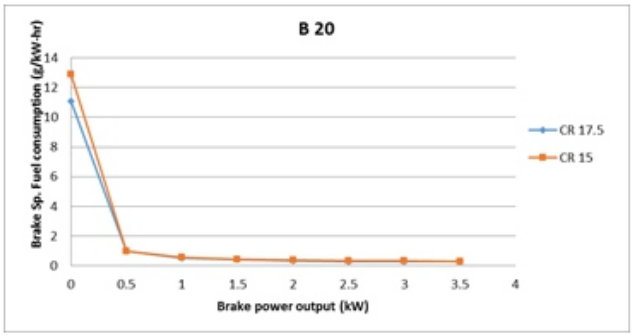

Fig-4.3. Comparison of Brake specific fuel consumptions v/s Brake power CR 17.5 & 15

5. BRAKE THERMAL EFFICIENCY

The effect of variation of brake power output on brake thermal efficiency at typical compression ratios of 17.5 and 15 for different biodiesel blends are shown in figures 5.1-5.3. The brake thermal efficiency of the engine increases with brake power output. It can be observed that brake thermal efficiency at different blends is comparable with diesel fuel. For CR of 17.5, the maximum values of brake thermal efficiencies were recorded to be 31.99 and 31.72 for biodiesel blends of B60 and B80, respectively. At CR values of 17.5 and 15, the maximum value of thermal efficiency was obtained at B20. Similar results were also reported by Ozsezen et al., 2009 [14].

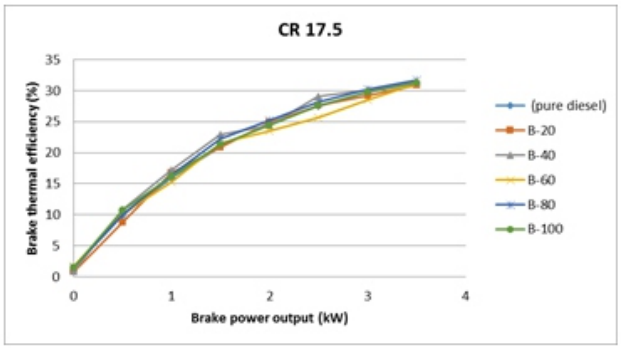

Fig-5.1. Brake thermal efficiency v/s Brake power output CR 17.5

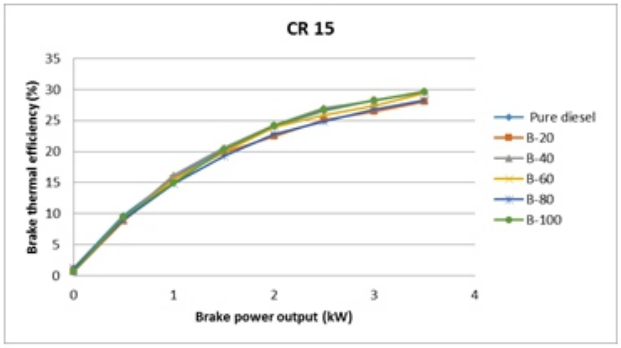

Fig-5.2. Brake thermal efficiency v/s Brake power output CR 15

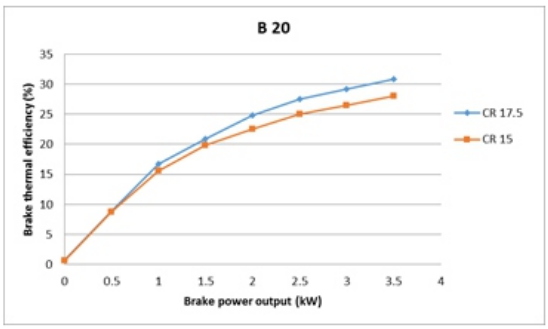

Fig-5.3. Brake thermal efficiency v/s Brake power output CR 17.5,15

6. EMISSION CHARACTERISTICS CARBON_MONOXIDE

Carbon monoxide is one of the arbitrate compound formed during the intermediate combustion stage of hydrocarbon fuels. CO formation depends on air fuel equivalence ratio, fuel type, combustion chamber design, starting of injection timing, injection pressure and speed. The effect of brake power output of engine on carbon-monoxide emission with various blends of biodiesel at two levels of compression ratio (i.e., 17.5 and 15) has been plotted in figure 6.1 and 6.2. At part load, pure diesel mode (with CR of 17.5) shows slightly lower level of CO emission than any biodiesel blends; at full loads, the biodiesel blends show better control on carbon-monoxide emissions. It may be expected due to complete oxidation. However, at CR of 15, the biodiesel shows slightly higher trends for CO emission than pure diesel mode. Similar trends were also accounted by Mazumdar and Agarwal, and Rao et al [15-16].

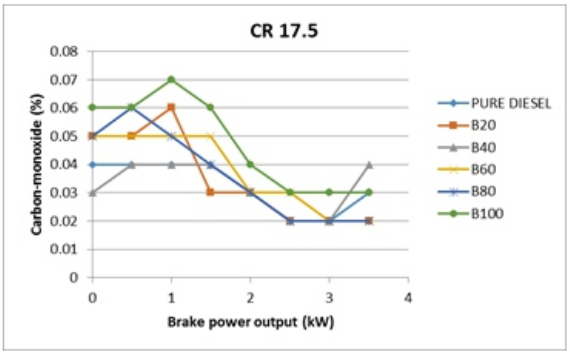

Fig. 6.1. Carbon monoxide v/s Brake power output CR 17.5

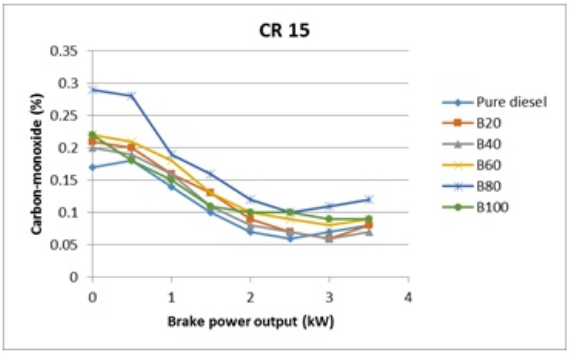

Fig. 6.2. Carbon monoxide v/s Brake power output CR 15

7. OXIDES OF NITROGEN EMISSION

The effect of variation of brake power output on NOx emissions at compression ratios of 17.5 and 15 for different biodiesel blends are shown in figure 7.1 and 7.2. NOx emissions increase with the increase in concentration of biodiesel in the blend and compression ratio. The emissions of nitrogen oxides from engine exhaust are highly dependent on oxygen concentration and thus, the combustion temperature. In general the NOx concentration varies linearly with the load of the engine. As the load increases, the overall fuel-air ratio increases resulting in an increase in the average gas temperature in the combustion chamber and hence NOx formation, which is sensitive to temperature increase. The NO_x obtained in this experiment follows the trends as described by Shirneshan [17].

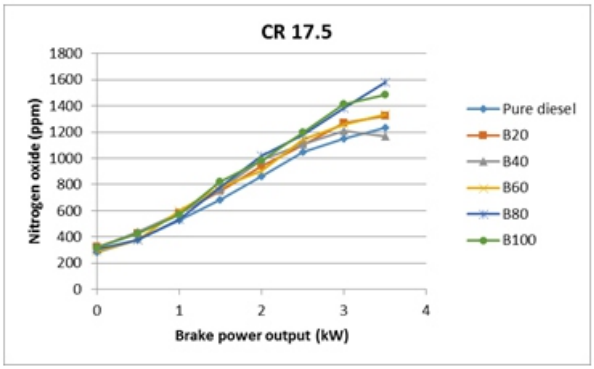

Fig. 7.1. Nitrogrnoxide v/s Brake power output CR 17.5

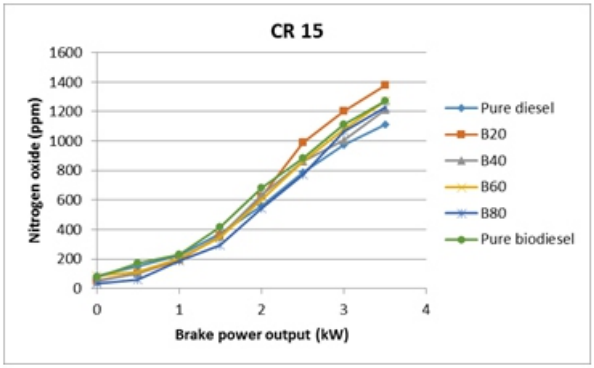

Fig. 7.2. Nitrogrnoxide v/s Brake power output CR 15

8. UNBURNT HYDRO-CARBON EMISSION

The effect of variation of brake power output on hydrocarbon emissions at compression ratios of 17.5 and 15 for different biodiesel blends are shown in figure 8.1 and 8.2**.** The emission of hydrocarbons (HC) tends to decrease with increasing the concentration of biodiesel in the blends as shown in figure. The reduction in the HC was linear with the addition of biodiesel for the blends tested. These reductions indicate a complete combustion of the fuel. Waste cooking oil biodiesel contains high oxygen content, which makes better combustion.

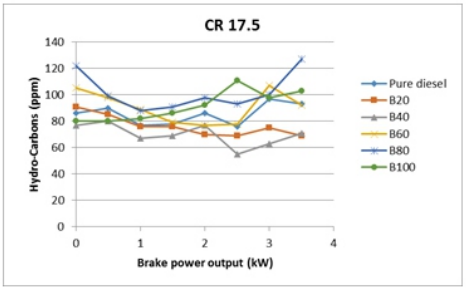

Fig. 8.1. Unburnt hydrocarbon v/s Brake power output CR 17.5

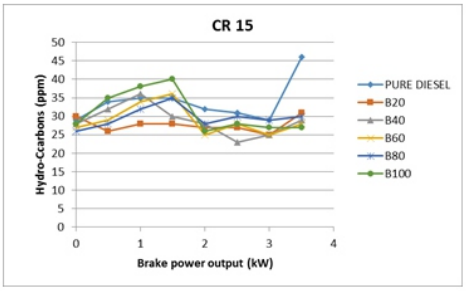

Fig. 8.2. Unburnt hydrocarbon v/s Brake power output CR 15

9. SMOKE OPACITY

The effect of variation of brake power output on smoke opacity at compression ratios of 17.5 and 15 for different biodiesel blends are shown in figure 9.1 and 9.2. Smoke opacity gives slightly increasing trends with brake power output. However, as either biodiesel concentration or compression ratio increases, the smoke opacity increases.

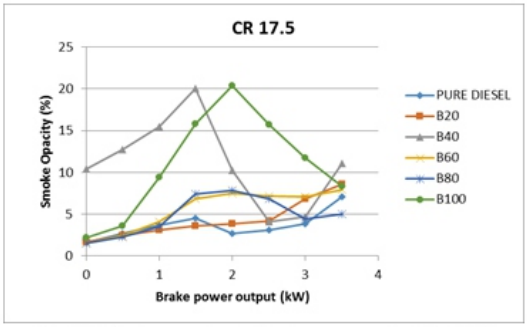

Fig. 9.1. Smoke opacity v/s Brake power output CR 17.5

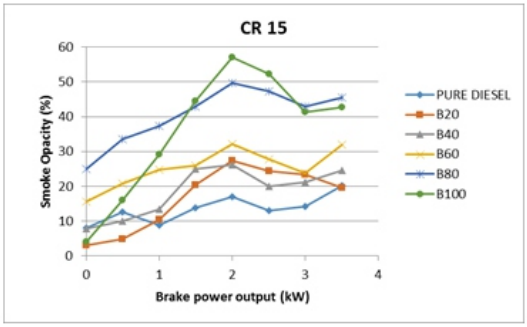

Fig. 9.2. Smoke opacity v/s Brake power output CR 15

10. CONCLUSIONS

In the present work, the thermal performance and emission characteristics of a variable compression ratio compression ignition engine fueled with biodiesel produced from waste cooking oil have been experimentally investigated and compared with base line diesel. The final inferences of the present work are summed up as follows.

1. The diesel engine can run satisfactorily on biodiesel and its blends with diesel without any engine modification.

2. The specific fuel consumption decreases with brake power output. The different blends of biodiesel fuel do not put any significant effect on specific fuel consumption. Specific fuel consumption is inversely proportional to compression ratio. It can be observed that for all blends of biodiesel, the brake specific fuel consumption was higher than conventional diesel. This pattern was due to the fact that biodiesel blends have a lower heating value than conventional diesel.

3. There is significant reduction in CO, unburnt hydrocarbons and smoke emissions for biodiesel and its blends as compared to conventional diesel. Whereas, NOx emission of waste cooking oil methyl esters is marginally higher than conventional diesel.

It can be summed up that in order to minimize the dependency on fossil fuels, waste cooking oil methyl ester is competent enough as conventional diesel, which will solve the problem of air pollution and utilization of waste cooking oil (by transesterifying it to produce biodiesel for compression ignition engine)

11. REFERENCES

[1] Intergovernmental Panel. "IPCC Fourth Assessment Report on Climate Change", 2009.
[2] Energy Information administration. "International Energy Outlook", Office of Integrated Analysis and Forecasting, U.S. Department of Energy, (2009).
[3] H. An, W.M. Yang, A. Maghbouli, J. Li, S.K. Chou, K.J. Chua. Performance, combustion and emission characteristics of biodiesel derived from waste cooking oil. Applied Energy 2013; 112: 493–499.
[4] Ministry of Petroleum and Natural gas, "Government of India", April 20, 2009.
[5] V. Bhardwaj, S. Sharma, S. K. Mohapatra, K. Kundu. Performance and emission characteristics of a C.I. engine fuelled with different blends of biodiesel derived from mustard oil. Proceedings of International Conference on Advances in Mechanical Engineering 2013 80-86.

[6] A. K. Agarwal. Biofuels (alcohols and biodiesel) applications as fuels for internal combustion engines. Progress in Energy and Combustion Science 2007; 33: 233–271.

[7] G. Velgutth. 1983. Performance of vegetable oil and their monsters as fuel for diesel engine. Society of Automotive Engineers 1983; Paper Number 831358.

[8] S.J. Clark, L. Wagner, M. D. Schrock, P.G. Piennar. Methyl and ethyl soybean esters as renewable fuels for diesel engine. Journal of the American Oil Chemists Society 1984; 61(10) 1632–1638.

[9] D. Agarwal, S. Sinha, A. K. Agarwal. 2006. Experimental investigation of control of Nox emissions in biodiesel fuelled compression ignition engine. Renewable Energy 2006; 31: 2356–2369.

[10] J.F. Sun, JA. Caton. TJ. Jacobs. 2010. Oxides of nitrogen emissions from biodiesel fuelled diesel engine. Progressive Energy Combustion Science 2010; 36: 677–95.

[11] L. Raslavicius and Z. Bazaras. Variation in oxygenated blend composition to meet energy and combustion characteristics very similar to diesel fuel. Fuel Process Technology 2010; 91: 1049-54.

[12] J. Bittle, B. Knight, T. Jacobs. 2009 The impact of biodiesel on injection timing and pulse width in a common rail medium-duty engine. Presented at the SAE power train fuels and lubricants fall meeting. San Antonio Texas SAE 01-2782.

[13] X. Meng, G. Chen, Y. Wang. Biodiesel production from waste cooking oil via alkali catalyst and its engine test. Fuel Process Technology 2008; 89: 851–857.

[14] A. N. Ozsezen, M. Canakci, A. Turkcan, C. Sayin. Performance and combustion characteristics of a DI diesel engine fuelled with waste palm oil and canola oil methyl esters. Fuel 2009; 88: 629-636.

[15] B. Mazumdar, A. K. Agarwal. Performance emission and combustion characteristics of biodiesel (Waste cooking oil methyl ester) fuelled IDI engine. Society of Automotive Engineers 2008; 01–13.

[16] G. L. N. Rao, S. Sampath, K. Rajgopal. Experimental studies on the combustion and emission characteristics of a diesel engine fuelled with used cooking oil methyl ester and its diesel blends. International Journal of Engineering and Applied Science 2008; 4: 64–70.

[17] A. Shirneshan. HC, CO, $CO_2$and NOx emission evaluation of a diesel engine fuelled with waste frying oil methyl ester 2013; 75: 292–297.

Thermodynamic Analysis of Different Desiccant Cooling Cycles

Ranjeet Kumar Jha[1], Durgesh Sharma[2]

[1]**Department of Mechanical Engineering,** Raj Kumar Goel Institute of Technology, Ghaziabad

ranjeetjha001@gmail.com

[2]**Department of Mechanical Engineering,** Raj Kumar Goel Institute of Technology, Ghaziabad

durgeshrsharma@gmail.com

Corresponding Author; Tel :+91-9999974132, 9891430333

A B S T R A C T

Desiccant cooling systems have been considered as an efficient method of controlling moisture in the air. These system consume less energy as compared with the Vapour Compression Systems In vapor compression refrigeration system a lot of energy is consumed to separate the moisture from air. In this work, thermodynamic analysis is applied on three different desiccant cooling cycles to get optimal performance.

Keywords—Desiccant Cooling 1; Dunkle Cycle 2; Second Law Efficiency 3,Thermodynamic Analysis 4.

1. INTRODUCTION

The moisture presents in air increase the cooling load of refrigeration system due to latent heat load of moisture. Desiccant cooling system is a environmentally friendly technology, which can be used to condition the air without the use of traditional refrigerants Desiccant absorbs the moisture from the process air and reduces the cooling load. It is becoming one of the most promising alternatives to conventional cooling systems.

.The reversible COP depends on the operating parameters and the analysis is based on certain operating conditions for the desiccant dehumidifier many researcher have studied first law and second law aspect of Desiccant Cooling systems. Lavan et al. [1] presented a general second law analysis of ventilation and recirculation cycle and introduced equivalent Carnot temperatures concept for evaluating reversible COP. Van den Bulck et al. [2] and Shen and Worek [3] considered desiccant dehumidifier in their studies. The latter considers the recirculation mode of the system operation and attempts to optimize the number of transfer units and the regeneration temperature of a dehumidifier based on the first and second laws of thermodynamics. Maclaine-Cross [4] considered a cycle with reversible components, which has infinite COP. Pons and Kodama [5] evaluated the various terms of internal and external entropy generation in ventilation mode and expressed relevant formulation with

respect to Carnot COP of the system. In the second part of the study, Kodama et al. [6] applied the formulation to an experimental unit and investigated the effects of certain operating parameters on the various terms of entropy generation. Wexing et al.[7] proposed a new type of modified Cross-Cooled Compact Dehumidifier (CCCD) and developed its mathematical model. The dehumidifier is constructed on the basic structure of plate fin heat exchanger with silica gel elaborately glued on all the metal surfaces of the process-flow channels.

2. FIRST LAW ANALYSIS OF THE SYSTEM

A schematic of the desiccant cooling system operating in ventilation mode is shown in Fig. 1. Air first enters into Desiccant wheel (DW), in which it is dehumidified and heated by the heat of adsorption. The hot dry air is then cooled sensibly in a Rotary Regenerator (RR). The process air is further cooled in an Evaporative Cooler (EC1) before being routed to the room. An equal flow of air is withdrawn from the room for regeneration. Regenerated air is first cooled in an Evaporative Cooler (EC2) and then preheated in the Rotary Regenerator by the warmer air in the process line. External heat is supplied to the regenerated air in a heating unit before passing through the Desiccant wheel , in which desiccant picks up moisture from the process air and transports to the hot regenerated air. The air leaves the Desiccant wheel hot and dry.. An ideal desiccant will dehumidify the air completely so that the specific humidity at the exit of Desiccant wheel will be zero.

$$w_2 = 0$$

where w_2 is specific humidity of the air at point 2

Processed air then pass through a Rotary Regenerator, it is a kind of counter flow heat exchanger. The effectiveness of heat exchanger may expressed as

$$\varepsilon_{RR} = \frac{(T2-T3)}{(T2-T6)} \qquad (1)$$

Where T2 , T3, and T6 are temperature at point 2, 3 and 6 as shown in the fig.

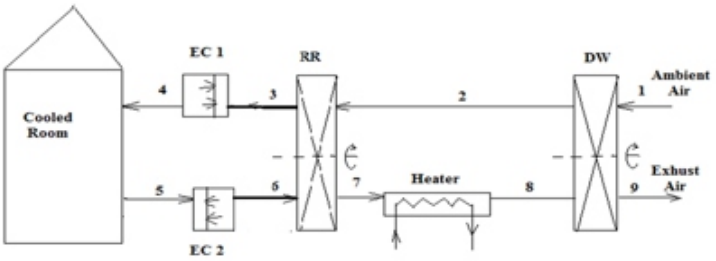

Fig.1. Desiccant Cooling System operating in ventilation mode.

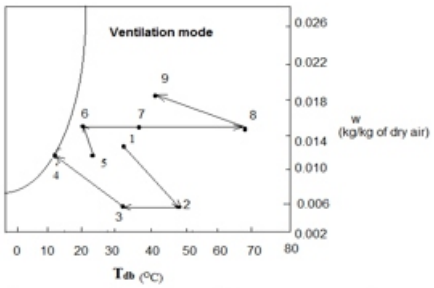

Fig.2. Psychrometric chart for system in ventilation mode.

The effectiveness of desiccant wheel may be expressed as

$$\varepsilon_{DW1} = ((T2 - T1))/((T8 - T1)) \qquad (2)$$

Another effectiveness relation for the desiccant wheel may be defined based on the dehumidification performance of the wheel with respect to the regeneration heat input, which may be expressed as

$$\varepsilon DW2 = (w2 - w1)hfg/((h8 - h1)) \qquad (3)$$

An energy balance on adiabatic Rotary Regenerator is given by

$$h2 - h3 = h7 - h6 \qquad (4)$$

The ideal operation for the Desiccant Wheel is based on the idea that the regeneration heat supplied to the regeneration air in the heater must not be more than latent heat needed for the complete dehumidification of ambient air in the Desiccant wheel. Then the regeneration heat may be calculated from.

$$Qreg = (w1 - w2)hfg = (w9 - w8)\, hfg \qquad (5)$$

where h_{fg} is the latent heat of vaporization for water. The enthalpy change of regeneration air across the Desiccant wheel must be equal to the heat input in the heater.

$$Qreg = (h8 - h9) \qquad (6)$$

The cooling capacity of system can be obtained by equation.

$$Qcool = (h5 - h4) \qquad (7)$$

The COP of a heat-driven cooling system is defined as the ratio of the cooling capacity to the heat input to the system. Then the thermal COP of this system becomes

$$\text{COP} = \frac{Qcool}{Qreg} = \frac{(h5 - h4)}{(h8 - h9)} \qquad (8)$$

The cycle operation as described above can also be applied to an open desiccant cooling system operating in recirculation mode and Dunkle modes. The schematics of these two modes are illustrated in Figure 3 and 5 and their psychrometric are shown in Figure 4 and 6 respectively. In recirculation mode, the room air is recalculated to the process line, while the ambient air is drawn into the regeneration line. Note that opposite to the ventilation mode, states 1 and 5 here represent the room and ambient states respectively.

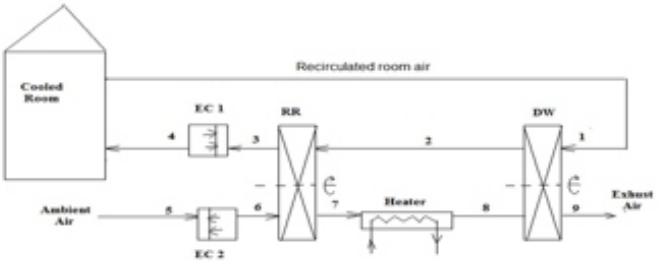

Fig.3. Desiccant Cooling System operating under Recirculation mode.

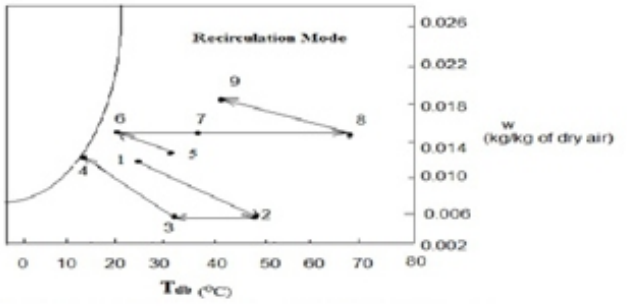

Fig.4.Psychrometric chart system in Recirculation mode.

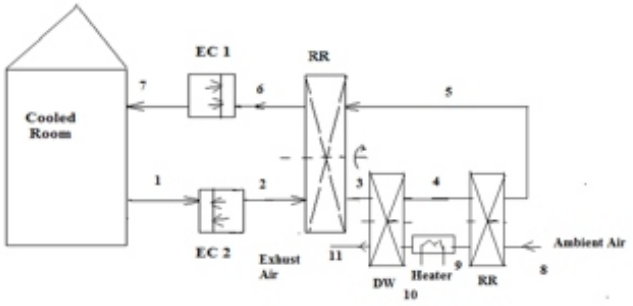

Fig.5. Desiccant Cooling System operating in Dukle mode.

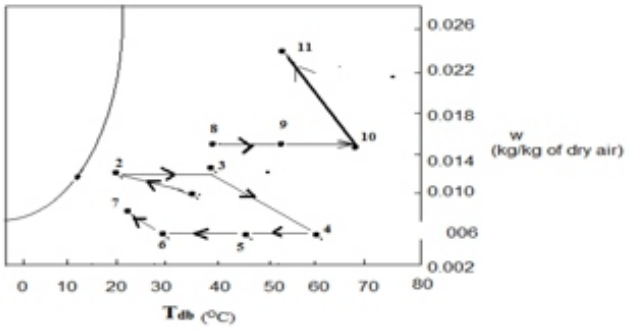

Fig.6.Psychrometric chart representation of system operation in Dunkle mode.

3. SECOND LAW ANALYSIS

The maximum COP of a heat-driven cooling system can be determined by assuming that the entire cycle is totally reversible. The cooling system would be reversible if the heat from the heat source were transferred to a Carnot heat engine, and the work output of this engine is supplied to a Carnot refrigerator to remove heat from the cooled space. The expressions for the work output from the Carnot heat engine, the cooling load of the Carnot refrigerator, and the Carnot COP of this reversible system may be calculated by equation 9.

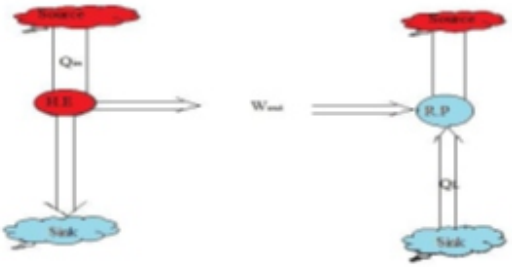

Fig 7 : Heat driven Cooling System

Now,

$$\frac{QL}{QIn} = \{TL|(TS - TL)\} \times \{(TS - TL)|TS\} \quad (9)$$

Where T_L and T_S are temperature of sink and source respectively . Heater is used as source and room space as a sink / evaporator and surrounding space is considered as condenser. So this cycle is three temperature cycle.

In case of desiccant cooling cycle in ventilation, dunkle and recirculation modes involve the mass transfer with the ambient and the room. Water is added in the evaporative coolers and to the process air in the room. We follow the approach given by the Lavan et al. [1], which is based on using equivalent Carnot Temperatures for the evaporator, condenser, and heat source.

4. CALCULATION OF EQUAVALENCE TEMPERATURE:

Heat Source:-

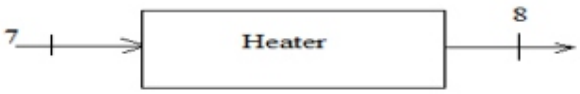

From Fist Law of Thermodynamics

$$QH = h8 - h7 \quad (10)$$

From Second Law of Thermodynamics

$$\frac{QH}{Ts} = (s8 - s7)$$

$$Ts = \frac{(s8-s7)}{(h8-h7)} \qquad (11)$$

Evaporator:-

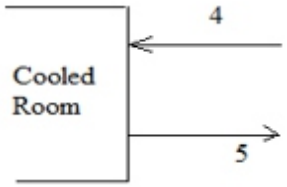

From First and Second Law of Thermodynamics

$$Te = \frac{(mah4-mah5+mw3hw)}{(mas4-mas5+mw3sw)} \qquad (12)$$

Condensing Unit:-

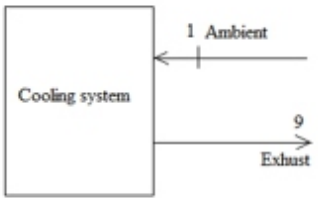

$$Tc = \frac{\{mah1-mah9-(mw1+mw2+mw3)hw\}}{\{mas1-mas9-(mw1+mw2+mw3)sw\}} \qquad (13)$$

Where mw3 is the rate of moisture added to process air in the cooled room, and hw and sw are the enthalpy and entropy of liquid water, respectively. It is clear that the reversible COP is functions of operating conditions.

The Second law efficiency is defined as it is the ratio of actual COP to the reversible COP.

$$\eta II = \frac{COP}{COPrev} \qquad (14)$$

5. EXPERIMENTAL SETUP:

To simulate three types of Desiccant Cooling system a simulation program has been developed in "C". The input parameter includes Initial conditions of air such as dry bulb temperature, Wet bulb, Relative humidity , specific humidity etc. The system will output different psychometric properties at different points in three cycles.

6. RESULTS AND DISCUSSION:

The calculated state properties of the system shown in Table .1.

Table 1 Calculated state properties of the system in Ventilation

State	T_{db} (^oC)	Twb	W	RH (%)	H (kJ/kg)	S (kJ/kg-K)
1	32.5	0.0094	19.4	0.329	56.01	5.803
2	45.5	0.0061	20.8	0.115	60	5.813
3	29.2	0.0061	16.4	0.237	46.48	5.769
4	16.8	0.0116	16.4	0.94	46.85	5.772
5	26.7	0.0116	19.5	0.53	56.5	5.805
6	20.4	0.01427	19.5	0.95	56.72	5.806
7	33.7	0.01427	23.6	0.435	70.43	5.852
8	63.8	0.01427	30.1	0.11	98.41	5.94
9	50.8	0.01747	28.9	0.227	95.39	5.933

The actual COPs of ventilation, Dunkle and recirculation cycles are 0.35, 0.390 and 0.401 by performing the Recirculation and Dunkle cycle in same by the same processes. The reversible COPs of these cycles are 3.12,4.7 and 5.24.

Performance data of the system at (Room T = 26.7 ^{0}C,RH = 50% ,Ambient T = 32.5 ^{0}C,RH = 32.9%)

Table 2 : Calculated Second law Efficiency

S.No	Parameter	Ventilation	Dunkle	Recirculation
1	COP	0.35	0.39	0.401
2	COPrev	3.12	4.7	5.24
3	ηII	11.21%	8.29%	7.60%

7. CONCLUSIONS:

The paper presents the thermodynamic analysis of three Desiccant Cooling Systems. A simulator was developed to obtain different psychrometric properties for given input parameters . Performance of three systems were measured in terms of second law efficiency. It was found that second law efficiency of ventilation cycle is more than the Dunkle and Recirculation Cycle .

8. REFERENCES

[1] Lavan Z, Monnier JB, Worek WM. Second law analysis of desiccant cooling systems. ASME J Sol Energy Eng 1982;104:229–36.

[2] Van Den Bulck E. The use of dehumidifiers in desiccant cooling and dehumidification systems. ASME J Heat Transfer 1986;108:684–92.

[3] Shen CM, Worek WM. The second law analysis of a recirculation cycle desiccant cooling system: cosorption of water vapor and carbon dioxide. Atmos Environ 1996;20:1429–35.

[4] I.L. Maclaine-cross, High performance adiabatic desiccant open cooling cycles, ASME Journal of Solar Energy Engineering 107 (1985) 102–104.

[5] M. Pons, A. Kodama, Entropic analysis of adsorption open cycles for air conditioning. Part 1: first and second law analyses, International Journal of Energy Research 24 (2000) 251–262.

[6] A. Kodama, W. Jin, M. Goto, T. Hirose, M. Pons, Entropic analysis of adsorption open cycles for air conditioning.Part 2: interpretation of experimental data, International Journal of Energy Research 24 (2000) 263–278.

[7] Weixing,Yi,Xiaoru,Xiugan,Study of a new modified cross-cooled compact solid desiccant dehumidifie, International Journal of Applied Thermal Engineering 28(2008) 2257-2266

Thermoeconomic Insulation for Environmental Sustainability

Radhey Shyam Mishra
Department Mechanical, Production & Industrial and Automobile Engineering
Delhi Technological University Delhi-110042 (INDIA)
Email: e-professor_rsmishra@yahoo.co.in,
Tel: +91-9891079311

A B S T R A C T

In this paper, simple economic analysis has been carried out for several insulating materials (such as cellular plastic, pearlite, corrugated asbestos, polyurethane rubber, styro-foam and rock-wool) with the objective in terms of most economic thickness. The various costs of insulations have been computed using explicit expressions & effect of various parameters i.e. thickness, heat transfer coefficients, temperature difference, payback period , interest rate for cylindrical geometry of pipes on the costs have been explained. It was observed that the most efficient and economic material comes to be cellular plastic of 0.031(W/m C) thermal conductivity.

KEYWORDS: Thermal Insulations Environmental Sustainability, Thermo-Economic Analysis

1. INTRODUCTION

For environmental sustainability, three main threats have been observed today in terms of the climate change driven by man-made emissions of gases which is referred as Global warming and also including the depletion of non-renewable resources along-with damage of the renewable resources and ecosystems is known as the resource depletion & also the largely dealt with under the Montreal Protocol known as the ozone depletion.

The ozone is also beneficial and harmful for mankind near the ground. The ozone forming is a result of chemical reactions involving due to traffic pollution & solar light, which may cause a number of respiratory problems. Although, in the stratosphere region, ozone is filtered out from incoming ultraviolet (UV) radiation from the Sun.

Without this ozone layer, life on earth would not have evolved in the way it has like an infection that grows more and more, Due to man made mad activities , the ozone destruction is increasing along with area of the ozone layer every day. The area of the ozone layer is also seasonally depleted of ozone is known as "ozone hole"Resource depletion is also defined in economic term relating to the exhaustion of raw materials within the region.

If these resources can be used of their beyond rate of replacement termed as considered as the resource depletion. The most important resources among others resources is a fossil fuel. If these fossil fuels were to run out now, there would not be a suitable replacement for them that are equally as efficient at producing the same amount of energy.

Energy conservation is a cost-effective ways for reducing the energy consumption through existing and improved technologies as well as through sound energy use practices is defined largely in terms of energy efficiency technologies and practices which can therefore be playing a significant role in the reducing the threat of global climate change. Therefore the judicious and effective use of renewable and non renewable energy for the optimizing (maximizing) the profits (minimize costs) for enhancing competitive positions.

Insulations are very important in the industrial & domestic applications. because it is reducing the heat energy losses from the atmosphere or heat gain in the cryogenic applications for conserving energy in terms of money saving through reducing the burden on energy resources & environment.

Mathematical modelling of thermal insulation has been carried to find the effect of various parameters such as payback period, rate of interest, heat transfer co-efficient and temperature differences in the cost of insulation, cost of heat losses and the total cost for a cylindrical surfaces and flat surfaces, it was observes that cellular plastic gives better properties of insulation than other materials. Insulations are very important in industrial applications & domestic use because it reduces heat losses to atmosphere or heat gain in cryogenic applications for conserving Energy in terms of money saving by reducing burden on energy resources & environment. The popular use of insulation is governed by economic considerations in terms of critical economic thickness. The method for finding the economic thickness of insulation is progressed significantly. Many researchers have laid down different methods of tackling thickness of insulation... M. Mc Chesney (1983) has calculated heat losses and developed thermal models which can be used for determining thickness of insulation. They have not considered if economic factors are not known so that heat losses considered without the fact that actual variable market conditions. Rubin (1982) has calculated thickness of insulation as a function of pipe size, fuel costs, pipe temperature based on wind speed of 12 km/hr with 15.5 degC ambient temperatures. Mishra (1984) has studied the effect of insulating materials on solar cooker thermal performance experimentally and calculated economic thickness theoretically by modifying running and inertial cost equations. In this paper, simple economic analysis has been carried out for five insulating materials such as cellular plastic, pearlite, corrugated asbestos, polyurethane rubber, styrofoam and rock-wool with the objective in terms of most economic thickness. The various costs of insulations are also

computed in terms of explicit expressions & effect of various parameters i.e. thickness, heat transfer coefficients, temperature difference, payback period , interest rate for cylindrical geometry of pipes on the costs have been explained. Insulations are very important in industrial applications & domestic use because it reduces heat losses to atmosphere or heat gain in cryogenic applications for conserving Energy in terms of money saving by reducing burden on energy resources & environment. The popular use of insulation is governed by economic considerations in terms of critical economic thickness .The various terms and quantities involved are as follows.

Length of pipe L, m, Outer radius of the insulation= r_o, m, Inner radius of the insulation (this is the same as the outer radius of the pipe) – r_i Thermal conductivity of insulation = K_c kcal/h $m^{2o}C$). Film coefficient at the outer surface on the insulation = h_0 (kcal/hr$m^{2o}C$). Pipe wall temperature (which is equal to the temperature of the inner surface of the insulation)=T_i (^oC)

Ambient temperature = T_o (^oC)

Cost of insulation = C' (Rs/m^3)

Life of insulation = n years

Number of working day in year=300 days

(i.e. 7200 hours)

Cost of heat energy =C_H (Rs/kcal)

Interest rate = I (Rs/year) (Rupees)

The inside heat transfer coefficient h_i is assumed to be large.

If (r_o-r_i) is the insulation thickness and ho the outer surface heat transfer coefficient, the overall heat transfer based on the inner radius of insulation can be expressed by following eq.(

) U_i= 1/((r_i/K_c)*ln(r_o/r_i) +(ri/(r_o*h_o)))

The rate of heat losses per year

Q=2*(3.14)*r_i*L U_i* (T_i-T_o) *24*300

=2*3.14*r_i*L U_i*(T_i-T_o)*(7.2 X1000) Kcal

Cost of heat loss = Q C_H)Rs/year)

If i is the fractional annual compound interest rate (compounded annually), the total present value of heat loss P_1 over the service life of the insulation (n years) is given by

Pi= Q C_H / (1+i) + Q C_H / $(1+i)^2$+

Q C_H / $(1+i)^3$ +Q C_H / $(1+i)^n$

Volume of insulation applied 3.14(r_o^2-r_i^2) L (m^3)

Present value of the insulation P_2= 3.14*(r_o^2-r_i^2) L C' (Rs)

The total present value or cost from Eqs( ) and ( ) is

P_T= Q C_H / (1+i) + Q C_H / $(1+i)^2$+

$Q C_H / (1+i)^3 \quad + Q C_H / (1+i)^n$

$3.14*(r_o^2 - r_i^2) L C' (Rs)$

The optimum insulation thickness is obtained by putting $dC_T/dR_o = 0$.

The development of a general expression for ro and therefore for the optimum insulation thickness (ro-ri) based on the expression for PT given by Eq.( ) is cumbersome. In this paper, simple economic analysis has been carried out for sixteen insulating materials such as Paper wood, cellotex, wood felt, Cork ,Mineral Fibre, Kapok Magnesia, Styrofoam Rook-wool Cement Polystyrene foam Silica aero-gel Rubber Fibre glass Plywood with the objective in terms of most economic thickness. The various costs of insulations have been computed using explicit expressions & effect of various parameters i.e. thickness, heat transfer coefficients, temperature difference, payback period , interest rate for cylindrical geometry of pipes on the costs have been explained. It was observed that the most efficient and economic material comes to be cellular plastic of 0.031(W/m C) thermal conductivity. For increasing the thermal conductivity, the total cost also increases as same value of temperature difference. For increase in payback period, the total cost also increases linearly. Increase in the heat transfer co-efficient the total cost of insulation first increases rapidly and stabiles for higher value of heat transfer co-efficient. Numerical computations was carried out for sixteen different insulation materials for a given pipe internal radius of 0.05m to find out most economic insulating materials.

2. RESULTS AND DISCUSSIONS

Materials	Thermal Conductivity(W/mK)	Economic thickness (mm)	Total cost (Rs.)
Plywood	0.12	105.1	497.5
Fibre glass	0.126	101.6	512
Rubber	0.14	106.1	544.7
PVC	0.017	104.7	567.1
Plastic	0.3	112.7	834.7
Silica aero-gel	0.024	61mm	1892
Polystyrene foam	0.025	60.4	1939.6
Cement	0.027	63.3	2030.3
Rook-wool	0.031	68	2205.8
Styrofoam	0.033	68.1	2290.2
Kapok Magnesia	0.035	70 mm	2372.6
Mineral Fibre	0.035	70 mm	2372.6
Cork Plastics	0.038	73	2493
Wood felt	0.045	74.2	2763.7
Cellotex	0.048	78.9	2870.4
Paper wood	0.072	89.2	3665.8

The most efficient economic material comes out to be cellular plastics. With increase in thermal conductivity the cost of insulation decreases and cost of heat losses increases and hence total cost also increases. Increases in interest rate leads to increases in total cost. For increase in heat transfer co-efficient, the total cost first increases rapidly and stabilizes for higher values of heat transfer co-efficient. For increases in temperature differences the total cost increase linearly. For increase in thermal conductivity the total cost also increases for same value of temperature differences. For increase in payback period the total cost of insulation also increases linearly

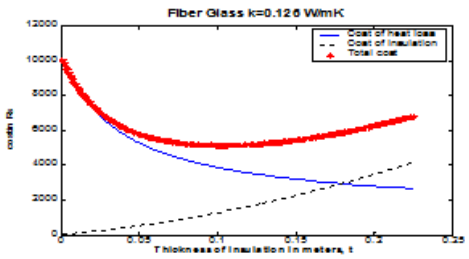

Fig-1a: Variation of various cost of Insulation with thickness of Insulation for fibre glass

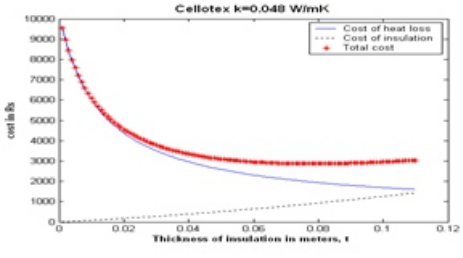

Fig-1b: Variation of various cost of Insulation with thickness of Insulation for cellotex

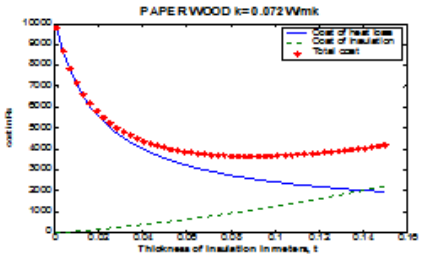

Fig-1c: Variation of various cost of Insulation with thickness of Insulation for paper wood

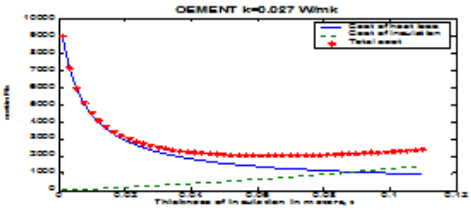

Fig-1d: Variation of various cost of Insulation with thickness of Insulation for cement

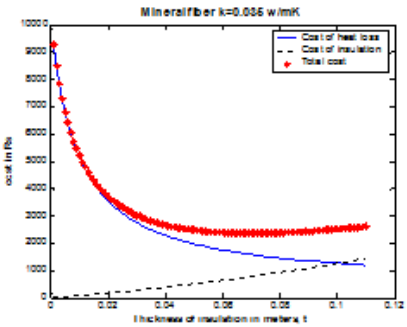

Fig-1(e) : Variation of various cost of Insulation with thickness of Insulation of mineral fibre

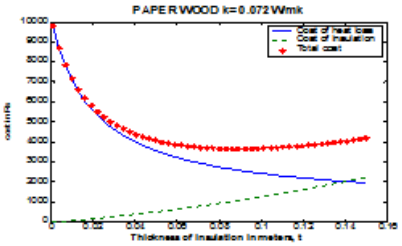

Fig-1(f) : Variation of various cost of Insulation with thickness of Insulation of paper wood

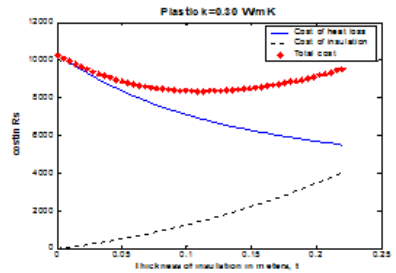

Fig-1(g) : Variation of various cost of Insulation with thickness of Insulation of plastic

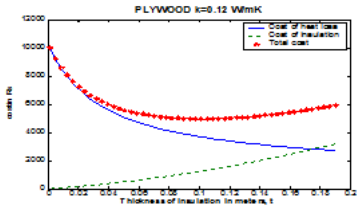

Fig-1(h) : Variation of various cost of Insulation with thickness of Insulation of paper-wood

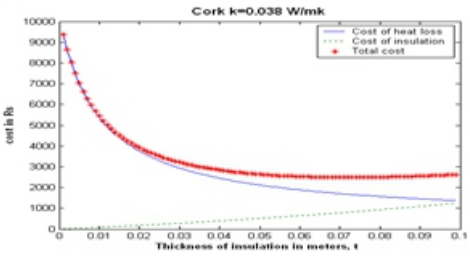

Fig-1(I) : Variation of various cost of Insulation with thickness of Insulation of cork

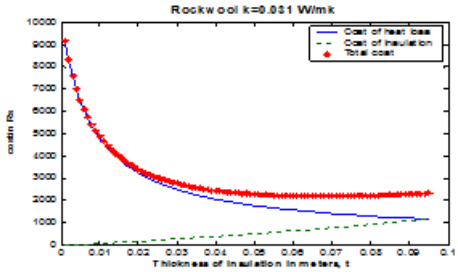

Fig-1(j) : Variation of various cost of Insulation with thickness of Insulation of roockwool

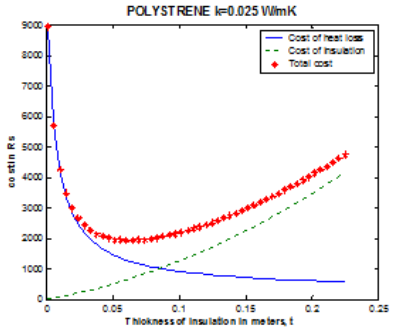

Fig-1(k) : Variation of various cost of Insulation with thickness of Insulation of polystyrene

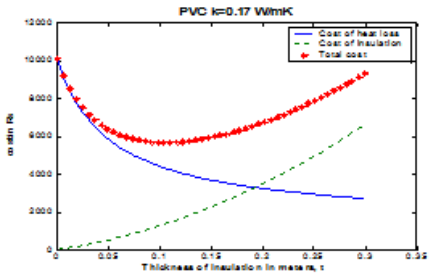

Fig-1(l) : Variation of various cost of Insulation with thickness of Insulation of pvc

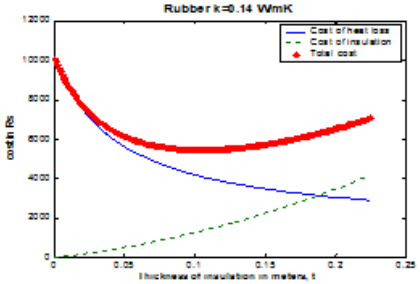

Fig-1(m): Variation of various cost of Insulation with thickness of Insulation of pvc

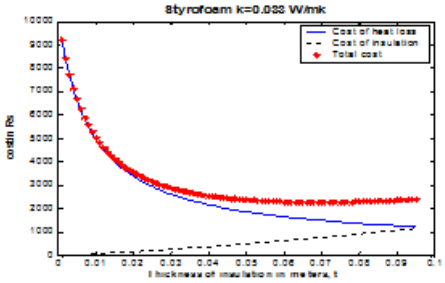

Fig-1(n): Variation of various cost of Insulation with thickness of Insulation of Styrofoam

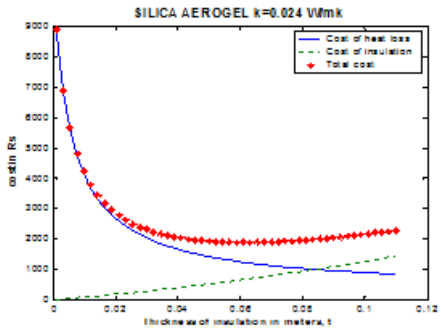

Fig-1(o): Variation of various cost of Insulation with thickness of Insulation of silica aerogel

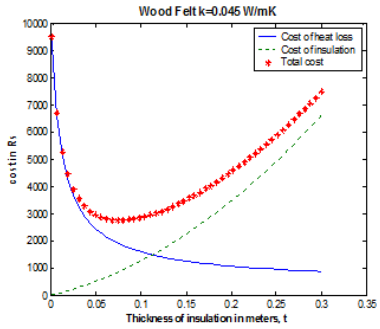

Fig-1(p): Variation of various cost of Insulation with thickness of Insulation of wood felt

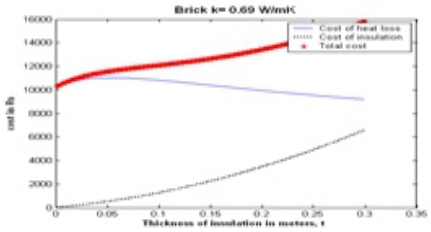

Fig-1 (q): Variation of cost with inner heat transfer coefficient of Insulation for fibre glass

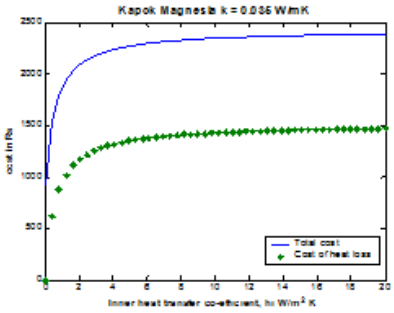

Fig-2 (a): Variation of cost with inner heat transfer coefficient of kook Megnesia

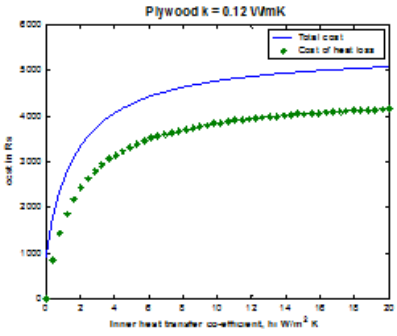

Fig-2 (b): Variation of cost with inner heat transfer coefficient of insulation of plywood

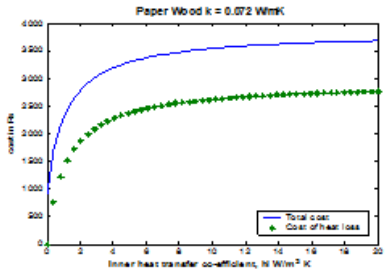

Fig-2 (c): Variation of cost with inner heat transfer coefficient Insulation for paper wood

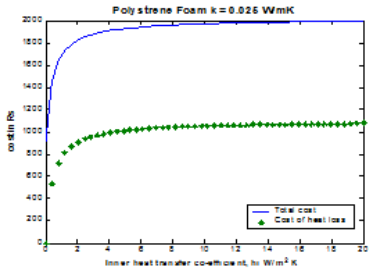

Fig-2 (d): Variation of cost with inner heat transfer coefficient Insulation for polystyrene foam

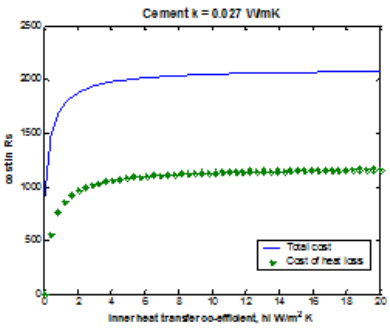

Fig-2 (e): Variation of cost with inner heat transfer coefficient Insulation for cement

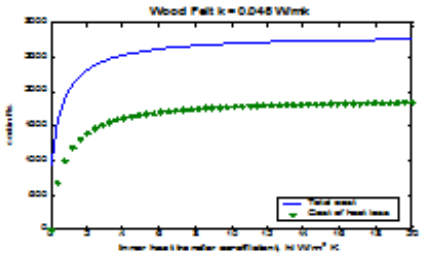

Fig-2 (f): Variation of cost with inner heat transfer coefficient of wood felt

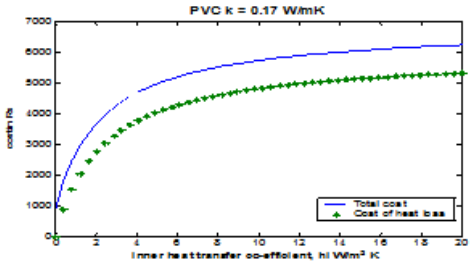

Fig-2 (g): Variation of cost with inner heat transfer coefficient Insulation of polystyrene Insulation of PVC

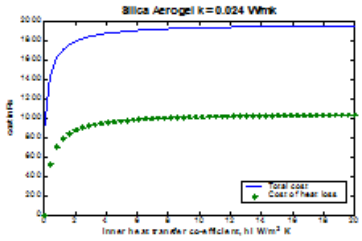

Fig-2 (h): Variation of cost with inner heat transfer coefficient silica aerogel

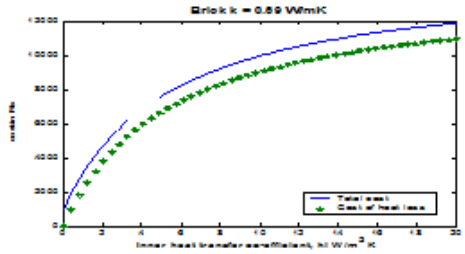

Fig-2 (i): Variation of cost with inner heat transfer coefficient of brick

3. CONCLUSIONS

The thermal analysis was done for the materials for sixteen different insulation materials for a given pipe internal radius of 0.05m and numerical computation was carried out to find out most economics materials. The following conclusions have been drawn:

1) The most efficient economic material comes out to be cellular plastic.

2) With increase in thermal conductivity the cost of insulation decreases and cost of heat losses increases and hence total cost also increases.

3) Increases in interest rate leads to increases in total cost.

4) For increase in heat transfer co-efficient the total cost first increases rapidly and stabilizes for higher values of heat transfer co-efficient.

5) For increases in temperature differences the total cost increase linearly.

6) For increase in thermal conductivity the total cost also increases for same value of temperature differences.

7) For increase in payback period the total cost of insulation also increases linearly

4. REFERENCES:

[1] Harrison MR (1977) Journal of chemical engineering. Vol. 84, page 61-63

[2] Malloy, JF(1969); Thermal insulation, Van Nostrand - Rainhold, Newyork.

[3] Mc Chesney, M (1981), Journal of chemical engineering Vol. 88, page 58-60

[4] Mishra, RS (1983); Effect of rural insulation on solar cooker, proc. International conference on renewable energy sources at Lahore (Pakistan) Page 391-399.

[5] Mishra, RS (1984); Evaluation of solar cooker thermal performance using different rural low cost insulating materials. International journal of Energy Research, John Wiley & Sons, NY, Vol 8 No.4, page 393-397

Mechanical Characterization of Epoxy Based Thermoses Polymer Composite With Sugar Cane Trash Natural Filler

Naveen J[1‡] & Veerendra Kumar A N[2]

[1]Research Scholar, Department of Mechanical Engineering Delhi Technological University, Delhi

naveen.j.murthy@gmail.com,

[2]Department of Mechanical Engineering, JSS Academy of Technical Education, Noida, INDIA

anvkumar38@gmail.com.

[‡]Corresponding author; Tel: +91 7503758119

ABSTRACT

Many researches are being carried out in the field of material science in order to develop new materials which can provide better mechanical properties, low in cost and does not harm our eco-system. Much attention of the scientists and engineers is towards reinforced polymer matrix composites in which a binder material is taken and reinforcement is done in the forms of particles, fibers and flakes or lamina in order to improve its mechanical properties. Reinforcement with the help of natural filler has many advantages like they are easily available, renewable, bio-degradable and has less weight to strength ratio. In this paper an attempt has been made to develop a composite material using epoxy as a binder material and sugarcane trash as reinforcement in particle form using compression molding process in different wt % i.e. 10%,15%,20% & 25%. Various tests like tensile test & bending test are performed on the prepared samples and analyzed in detail.

Keywords- Epoxy, Natural filler- Sugarcane Trash, Compression Molding Process, Tensile Test, Bending Test.

1. INTRODUCTION

Nowadays composite materials are used in myriad applications in engineering structures that includes automobiles, airplanes, spacecraft, bridges building, sports equipments etc. Composite materials are used tremendously in industries. Application of composite material was started in aerospace industry in late 1970's but today it is booming inevitably. Also in automobile industries, due to progresses in technology composites are replacing metallic automotive parts [1].

Natural filler has gained importance as a reinforcement material in the reinforced polymer matrix composite due to increasing concern towards environment. Using natural fillers as additives for composite materials gives a satisfactory result for improving their performance and applications due to biodegradability, abundance, low cost and high specific strength. It is also beneficial due to low density, mass of composite is reduced by the use of natural filler.[2]

Sugarcane trash is a abundantly available waste material which can be used as a natural filler material in the reinforced polymer matrix composites. It is obtained from the agricultural waste and can be treated as filler material [3].

Epoxy resins are one of the important class of thermosetting polymers which are widely used as a matrix for reinforced polymer composite materials and also as structural adhesive. It improves resistance to fatigue and micro-cracking and does not forms volatile products.[4]

According to latest studies on properties and preparation of reinforced polymer matrix composites using natural filler like sugarcane, bamboo, jute, kenaf, pineapple were carried out.[4][5][6] In recent practice it is seen that natural fiber composites are used in both interior and exterior parts in car manufacturing, this fulfills two motives of companies i.e. to reduce the overall weight of vehicle which increases the fuel efficiency and sustainability of manufacturing process is also increased. It is accomplished in many companies like Mercedes benz, Daimler Chrysler and Toyota and also scoping to expand the use of natural fiber composites.

1.1. Objective

The main objective is to study and evaluate the mechanical and physical properties of sugarcane trash as a reinforcement material in the epoxy resin matrix. A series of composite material will be developed by varying the wt% of sugarcane trash i.e. 10%, 15%, 20% & 25%. and testing will be performed in order to analyze the mechanical properties of the developed material. The various tests includes tensile test & bending test.

2. MATERIAL USED

2.1. Sugarcane

Sugarcane trash is an abundantly available waste material which can be used as a natural filler material in the reinforced polymer matrix composites. It is obtained from the agricultural waste and can be treated as filler material. It is obtained by crushing and extraction of juice from the sugarcane, the residue left out in the form of fiber is converted into particle form which is generally grey-yellow to pale green in color. The two main constituents of sugarcane trash are cellulose & hemi-cellulose and lignin. Cellulose and hemi-cellulose contributes about 70% of total chemical constituent and lignin acts as a binder material for the cellulose fibers[7]. Some other abundantly available natural fillers are jute, sisal, coir, ramie, bamboo, banana etc. These fillers are used as reinforcement with a binder material to develop newer materials. The selection of the natural filler should be such that it has excellent chemical bonding with the binder material i.e. the affinity of bonding should be good between reinforcement material and binder material.[8]

2.2. Epoxy

Epoxy resins are one of the important class of thermosetting polymers which are widely used as a matrix for reinforced polymer composite materials and also as structural adhesive. It is amorphous, highly cross-linked polymer which possesses various desirable properties like high tensile strength and modulus, good thermal and chemical resistance, dimensional stability, excellent adhesion to different materials and negligible shrinkage.[4]

2.3. Hardener (Araldite HY 951)

Hardeners are used to enhance the physical properties of epoxy resins such as adhesion, impact strength and to alter the viscosity of the polymer matrix. It also improves the life, lower exotherm and reduce shrinkage.

3. MECHANICAL, PHYSICAL PROPERTIES AND TESTINGS

3.1. Density and Particle size of sugarcane trash

Sugarcane is obtained by crushing and extraction of juice from the sugarcane, the residue left out in the form of fiber is converted into particle form by spray dryer method. It is a method of producing a dry powder from liquid or slurry by rapidly drying with a hot gas. All spray dryers are some type of atomizer to disperse the liquid or slurry into a controlled drop size spray. The obtained particle size (in mm) of the sugarcane trash was 2.224mm in length and 0.479 mm in width with projection microscopic method. The density of sugarcane trash was 0.904 gm/cm3 which was obtained by in-house method.

3.2. Tensile Strength

Tensile strength of a material is obtained by tension test in which specimen is prepared as shown in Figure 1 and subjected to uni-axial load until fracture in order to find out various mechanical properties of the specimen such as ultimate tensile strength, yield strength etc on tensile testing machine, shown in Figure 3. The tension test specimen has two shoulders and a gage in between, shoulders are made large so that it can be gripped firmly in the tension test machine and gage section has smaller area so that the deformation and failure can occur in this area.[9]. The specimen has been prepared as per ASTM D 638

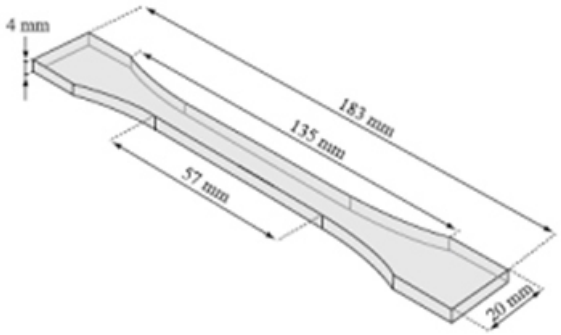

Figure 1. Tensile Test Specimen (Dog-Bone Type) line diagram

Figure 2. Tensile Testing Machine

3.3. Bending Test

A three point bending test is performed on the specimen as shown in Figure 3 as per ASTM D 790, to find out the flexural stress of the material. The specimen is placed on two supporting pins and set distance apart and the third pin is lowered from above at constant rate until the specimen gets fracture[10][14] the mounting of the specimen is shown in the Figure 4. For rectangular sample under a load in three point bending set-up, the formula for calculating the flexural stress is given by Eq (1):

$$S_f = 3PL / 2bd^2 \quad (1)$$

S_f – flexural stress

P – Load at fracture point

L – Length of support span

b – Width of the specimen

d – Thickness of the specimen.

The span length is taken as 12.6 cm

Figure-3. Beam of Material Under Bending

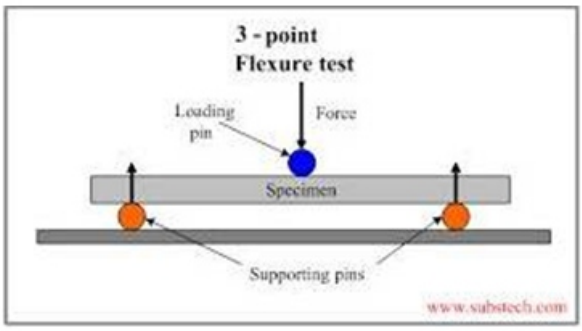

Figure 4. Flexural Testing Machine

4. EXPERIMENT PROCEDURE

4.1. Design and preparation of mould

For mould preparation a ceramic plate was used over which (mould of dimension 25cm × 20cm × 0.4cm) was made with overlapping twice the double sided tape of thickness 2mm. A thin sheet is placed in mould first and then epoxy mixture is poured into mould [11] as shown in below Figure 5

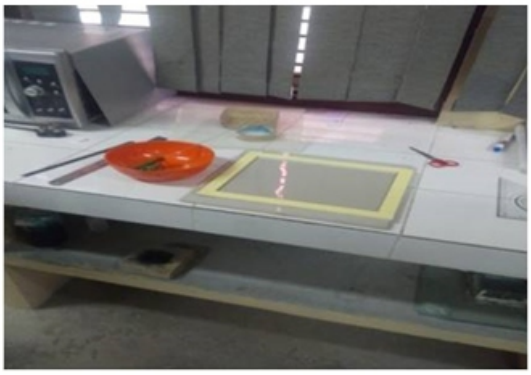

Figure 5. Design of Mould

4.2. Preparation of pure epoxy resin

Epoxy resin and hardener were mixed in ratio of 10:1 after separately weighting them an electronic balance [13].

4.3. Preparation of composite specimen

Epoxy mixture is taken in the bowl and thoroughly mixed and added sugarcane particle in mixture according to volume fraction and then continue mixing till its solidification states as shown in Figure 6. Gradually poured the mixture in the mould and spread it in the mould thoroughly. The mould was filled to brim and was placed on flat surface. Sharp needle was used for punching to remove the excess bubble. Finally covered the mould with OHP sheet and pressure exerted on it by putting weight [16]. Left the mould to cure for 24 hours under normal atmospheric condition. Finally, composite was taken out from mould and stored safely for further test. [15]

Figure 6. Mixing of Epoxy resin and Sugarcane Trash

5. RESULT AND DISCUSSION

5.1. Tensile Strength Dimension of specimen = (18.3cm x 2cm x 0.4cm)

Parallel length= 1cm,
Gage length= 9cm,
Grip width= 3cm
The Table 1 below shows the average value of the tensile strength for three specimens for each wt % of filler and corresponding graphical representation as shown in Figure 7. The tensile strength of the parent material without filler is found to be 22.15MPa.

Table 1- Tensile Strength

S.No	Filler content (wt%)	Tensile Strength (MPa)
1	Sample 1, 10%	27.17
2	Sample 2, 15%	31.67
3	Sample 3, 20%	26.21
4	Sample 4, 25%	25.23

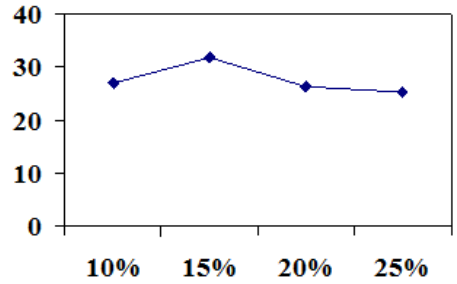

Figure 7. Filler content (wt%) v/s Tensile Strength (MPa)

5. 2. Percentage of Elongation

The Table 2 below shows the average value of the tensile strength for three specimens for each wt % of filler and graphical representation for the same shown, in Figure 8.

Table-2 Percentage of Elongation obtained in tension test

SNo	Filler content (wt %)	Elongation %
1	Sample 1, 10%	1.58
2	Sample 2, 15%	1.43
3	Sample 3, 20%	1.3
4	Sample 4, 25%	1.28

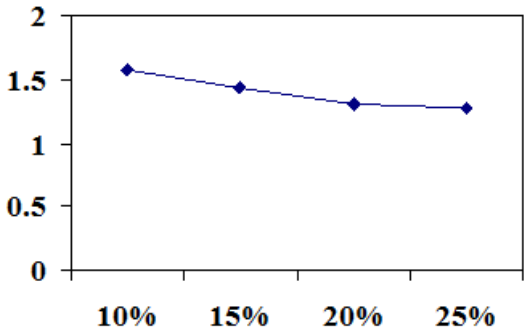

Figure 8. Filler content (wt%) v/s Percentage of Elongation

5.3. Flexural Strength

Dimension of specimen = (12.6cm x 1.3cm x 0.4cm).
The flexural strength of the parent material without filler is fount to be 40.5MPa.

The Table 3 below shows the average value of flexural strength for three specimens for each wt% of filler and corresponding graphical represntation shown, in Figure 9.

Table-3 Flexural Strength

SNo	Filler content (wt %)	Flexural Strength (Mpa)
1	Sample 1, 10%	55.2
2	Sample 2, 15%	46.16
3	Sample 3, 20%	46.08
4	Sample 4, 25%	49.81

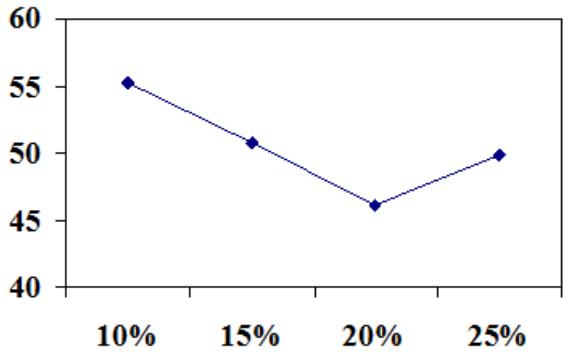

Figure 9. Filler content (wt%) v/s Flexural Strength (MPa)

6. CONCLUSION

(i) As we get the density of sugarcane trash as 0.904 gm/cm^3 so sugarcane trash can be used as filler material because adding this will reduce the weight of the specimen.

(ii) Developed composite having 15% filler is showing good results in tensile test.

(iii) Developed composite having 10% filler by weight is showing good results in elongation.

(iv) It is observed that when percentage sugarcane trash increases, tensile strength of the specimen increases upto 15% and then it shows decline. The elongation% decreases as the percentage of sugarcane trash increases.

(v) The flexural strength comes out to be maximum at 10% filler content and then it start decreasing when the percentage of filler content increases.

7. REFERENCE

[1] Fuchs, E. R., Field, F. R., Roth, R., & Kirchain, R. E. (2008). Strategic materials selection in the automobile body: Economic opportunities for polymer composite design. Composites Science and Technology, 68(9), 1989-2002.

[2] Taj, Saira, Munawar Ali Munawar, and Shafiullah Khan. "Natural fiber-reinforced polymer composites." Proceedings-Pakistan Academy of Sciences 44, no. 2 (2007): 129.

[3] Begum, K., & Islam, M. (2013). Natural fiber as a substitute to synthetic fiber in polymer composites: a review. Research Journal of Engineering Sciences.

[4] Sapuan, S. M., M. Harimiand, and M. A. Maleque. "Mechanical properties of epoxy/coconut shell filler particle composites." Arabian Journal for Science and Engineering 28, no. 2 (2003): 171-182.

[5] Raju, G. U., and S. Kumarappa. "Experimental study on mechanical properties of groundnut shell particle-reinforced epoxy composites." Journal of Reinforced Plastics and Composites 30, no. 12 (2011): 1029-1037.
[6] Deka, Harekrishna, Manjusri Misra, and Amar Mohanty. "Renewable resource based ‘‘all green composites’’ from kenaf biofiber and poly (furfuryl alcohol) bioresin." Industrial Crops and Products 41 (2013): 94-101.
[7] Wirawan, Riza, S. M. Sapuan, Robiah Yunus, and Khalina Abdan. "Properties of sugarcane bagasse/poly (vinyl chloride) composites after various treatments." Journal of Composite Materials 45, no. 16 (2011): 1667-1674.
[8] Luz, S. M., J. Del Tio, G. J. M. Rocha, A. R. Gonçalves, and A. P. Del'Arco. "Cellulose and cellulignin from sugarcane bagasse reinforced polypropylene composites: Effect of acetylation on mechanical and thermal properties."Composites Part A: Applied Science and Manufacturing 39, no. 9 (2008): 1362-1369
[9] Yang, Han-Seung, Hyun-Joong Kim, Jungil Son, Hee-Jun Park, Bum-Jae Lee, and Taek-Sung Hwang. "Rice-husk flour filled polypropylene composites; mechanical and morphological study." Composite Structures63, no. 3 (2004): 305-312.
[10] Rao, K. Murali Mohan, K. Mohana Rao, and AV Ratna Prasad. "Fabrication and testing of natural fibre composites: Vakka, sisal, bamboo and banana."Materials & Design 31, no. 1 (2010): 508-513.
[11] Shenoy, Srinivas, Suhas Y. Nayak, Ayush Prakash, Ankit Awasthi, and Rishabh Singh Kochhar. "Interlaminar shear and flexural properties of E-glass/jute reinforced polymer matrix Composites." (2015): 26-31.
[12] Sen, Tara, and HN Jagannatha Reddy. "Flexural strengthening of RC beams using natural sisal and artificial carbon and glass fabric reinforced composite system." Sustainable Cities and Society 10 (2014): 195-206.
[13] Kranthi, Ganguluri, and Alok Satapathy. "Evaluation and prediction of wear response of pine wood dust filled epoxy composites using neural computation." Computational Materials Science 49, no. 3 (2010): 609-614.
[14] Sapuan, S. M., A. Leenie, Mohamed Harimi, and Yeo Kiam Beng. "Mechanical properties of woven banana fibre reinforced epoxy composites."Materials & Design 27, no. 8 (2006): 689-693.
[15] Yu, Long, Katherine Dean, and Lin Li. "Polymer blends and composites from renewable resources." Progress in polymer science 31, no. 6 (2006): 576-602.
[16] Tatara, R. A., S. Suraparaju, and K. A. Rosentrater. "Compression molding of phenolic resin and corn-based DDGS blends." Journal of Polymers and the Environment 15, no. 2 (2007): 89-95.

Instructions for Authors

Essentials for Publishing in this Journal

1 Submitted articles should not have been previously published or be currently under consideration for publication elsewhere.

2 Conference papers may only be submitted if the paper has been completely re-written (taken to mean more than 50%) and the author has cleared any necessary permission with the copyright owner if it has been previously copyrighted.

3 All our articles are refereed through a double-blind process.

4 All authors must declare they have read and agreed to the content of the submitted article and must sign a declaration correspond to the originality of the article.

Submission Process

All articles for this journal must be submitted using our online submissions system. http://enrichedpub.com/ . Please use the Submit Your Article link in the Author Service area.

Manuscript Guidelines

The instructions to authors about the article preparation for publication in the Manuscripts are submitted online, through the e-Ur (Electronic editing) system, developed by **Enriched Publications Pvt. Ltd**. The article should contain the abstract with keywords, introduction, body, conclusion, references and the summary in English language (without heading and subheading enumeration). The article length should not exceed 16 pages of A4 paper format.

Title

The title should be informative. It is in both Journal's and author's best interest to use terms suitable. For indexing and word search. If there are no such terms in the title, the author is strongly advised to add a subtitle. The title should be given in English as well. The titles precede the abstract and the summary in an appropriate language.

Letterhead Title

The letterhead title is given at a top of each page for easier identification of article copies in an Electronic form in particular. It contains the author's surname and first name initial .article title, journal title and collation (year, volume, and issue, first and last page). The journal and article titles can be given in a shortened form.

Author's Name

Full name(s) of author(s) should be used. It is advisable to give the middle initial. Names are given in their original form.

Contact Details

The postal address or the e-mail address of the author (usually of the first one if there are more Authors) is given in the footnote at the bottom of the first page.

Type of Articles

Classification of articles is a duty of the editorial staff and is of special importance. Referees and the members of the editorial staff, or section editors, can propose a category, but the editor-in-chief has the sole responsibility for their classification. Journal articles are classified as follows:

Scientific articles:

1. Original scientific paper (giving the previously unpublished results of the author's own research based on management methods).

2. Survey paper (giving an original, detailed and critical view of a research problem or an area to which the author has made a contribution visible through his self-citation);

3. Short or preliminary communication (original management paper of full format but of a smaller extent or of a preliminary character);

4. Scientific critique or forum (discussion on a particular scientific topic, based exclusively on management argumentation) and commentaries. Exceptionally, in particular areas, a scientific paper in the Journal can be in a form of a monograph or a critical edition of scientific data (historical, archival, lexicographic, bibliographic, data survey, etc.) which were unknown or hardly accessible for scientific research.

Professional articles:

1. Professional paper (contribution offering experience useful for improvement of professional practice but not necessarily based on scientific methods);
2. Informative contribution (editorial, commentary, etc.);
3. Review (of a book, software, case study, scientific event, etc.)

Language

The article should be in English. The grammar and style of the article should be of good quality. The systematized text should be without abbreviations (except standard ones). All measurements must be in SI units. The sequence of formulae is denoted in Arabic numerals in parentheses on the right-hand side.

Abstract and Summary

An abstract is a concise informative presentation of the article content for fast and accurate Evaluation of its relevance. It is both in the Editorial Office's and the author's best interest for an abstract to contain terms often used for indexing and article search. The abstract describes the purpose of the study and the methods, outlines the findings and state the conclusions. A 100- to 250- Word abstract should be placed between the title and the keywords with the body text to follow. Besides an abstract are advised to have a summary in English, at the end of the article, after the Reference list. The summary should be structured and long up to 1/10 of the article length (it is more extensive than the abstract).

Keywords

Keywords are terms or phrases showing adequately the article content for indexing and search purposes. They should be allocated heaving in mind widely accepted international sources (index, dictionary or thesaurus), such as the Web of Science keyword list for science in general. The higher their usage frequency is the better. Up to 10 keywords immediately follow the abstract and the summary, in respective languages.

Acknowledgements

The name and the number of the project or programmed within which the article was realized is given in a separate note at the bottom of the first page together with the name of the institution which financially supported the project or programmed.

Tables and Illustrations

All the captions should be in the original language as well as in English, together with the texts in illustrations if possible. Tables are typed in the same style as the text and are denoted by numerals at the top. Photographs and drawings, placed appropriately in the text, should be clear, precise and suitable for reproduction. Drawings should be created in Word or Corel.

Citation in the Text

Citation in the text must be uniform. When citing references in the text, use the reference number set in square brackets from the Reference list at the end of the article.

Footnotes

Footnotes are given at the bottom of the page with the text they refer to. They can contain less relevant details, additional explanations or used sources (e.g. scientific material, manuals). They cannot replace the cited literature.
The article should be accompanied with a cover letter with the information about the author(s): surname, middle initial, first name, and citizen personal number, rank, title, e-mail address, and affiliation address, home address including municipality, phone number in the office and at home (or a mobile phone number). The cover letter should state the type of the article and tell which illustrations are original and which are not.

Address of the Editorial Office:

Enriched Publications Pvt. Ltd.
S-9,IInd FLOOR, MLU POCKET,
MANISH ABHINAV PLAZA-II, ABOVE FEDERAL BANK,
PLOT NO-5, SECTOR -5, DWARKA, NEW DELHI, INDIA-110075,
PHONE: - + (91)-(11)-45525005

Notes: